

# Persistence of a reef fish metapopulation via network connectivity: theory and data

Allison G. Dedrick<sup>a,\*1</sup>

Katrina A. Catalano<sup>a</sup>

Michelle R. Stuart<sup>a</sup>

J. Wilson White<sup>b</sup>

Humberto R. Montes, Jr.<sup>c</sup>

Malin Pinsky<sup>a</sup>

a. Department of Ecology Evolution and Natural Resources, Rutgers University, 14 College Farm Road, New Brunswick, NJ 08901 USA;

b. Department of Fisheries and Wildlife, Coastal Oregon Marine Experiment Station, Oregon State University, Newport, OR 97365 USA;

c. Visayas State University, Pangasugan, Baybay City, 6521 Leyte, Philippines

\* Corresponding author; e-mail: agdedrick@gmail.com

1. Current address: Stanford Woods Institute for the Environment, Stanford University, Stanford, CA 94305 USA.

**Running title:** (45 characters including spaces) Empirical metapopulation persistence

**Keywords:** metapopulation dynamics, self-persistence, network persistence, dispersal kernel, *Amphiprion clarkii*, connectivity (5/10)

**Type of article:** Letters

**Statement of authorship:** Conceptualization, Methodology: MLP, JWW, and AGD. Investigation: MLP, MRS, KAC, and AGD. Software, Formal Analysis, Visualization: AGD. Resources: HRM. Data Curation: MRS. Writing - Original Draft: AGD. Writing - Review and Editing: AGD, KAC, MRS, JWW, HRM, MLP. Supervision, Funding Acquisition: MLP.

**Data accessibility statement:** Sample data, metadata, GIS data, and analysis code is stored in a GitHub repository and will be made public after acceptance. The repository will be archived with a DOI through Zenodo.

**Words in the abstract:** 130/150

**Words in the main text:** about 5500

**Number of references:** 62

**Number of main figures, tables, and text boxes:** 6

**Number of supplementary figures, tables, and text boxes:** 19

## Acknowledgements

We thank Visayas State University for providing scientific and logistical support during our field sampling in Leyte, Philippines, as well as the municipalities of Bay Bay City and Albueria. We particularly thank Geralde Sucano, Jennifer Hoey, Patrick Flanagan, Joyce Ong, Apollo Lizano, Cecil Bantiles, Rodney Silvado, Beverlito Montalban, Teresita Idara, Rogello Nicanor, Liza Espinosa, Shem San Jose, Noel Alquino, Carlos Balansuna, Froilan Beas, Danilo Marine, Tony Nahacky, and Arturo Bastasa. For financial support, we thank Rutgers School of Environmental and Biological Sciences, NSF #OCE-1430218, an Alfred P. Sloan Research Fellowship, and an ORAU Ralph E. Powe Junior Faculty Enhancement award. This is publication number ## of PISCO, the Partnership for Interdisciplinary Study of Coastal Oceans, funded primarily by the David and Lucile Packard Foundation.

## Abstract

Determining whether a metapopulation can persist requires an understanding of both demographic parameters and connectivity among patches. This is well understood in theory but has proved challenging to test empirically. We assessed persistence for

a network of patches along a coastline in a metapopulation of yellowtail anemonefish (*Amphiprion clarkii*) using seven years of annual sampling data along 30 km of coastline. Despite stable population sizes through time and sufficient production of surviving offspring for replacement, the spatial pattern of connectivity made the metapopulation unlikely to persist in isolation. To persist, the metapopulation would need higher fecundity or would need to retain essentially all of the recruits it produced. This assessment of persistence in a marine metapopulation shows that stable abundance alone is not an indicator of persistence, emphasizing the necessity of untangling demographic and connectivity processes to understand metapopulation dynamics. (130/150 words)

## Introduction (622 words)

The dynamics and persistence of metapopulations depend both on connectivity  
3 among patches and on demographic rates within each patch (Hastings and Botsford, 2006; Hanski, 1998). For marine species, connectivity among habitat patches primarily occurs during planktonic larval stages when individuals are hard to track  
6 and are able to travel long distances with ocean currents. Because larval connectivity has been perceived to be the greatest uncertainty in these systems, research has centered on quantifying that component (reviewed by White et al., 2019). More  
9 recently, it has become apparent that variation in demographic rates among patches is an equally uncertain aspect of marine metapopulation dynamics (Hameed et al., 2016; White and Samhouri, 2011). Given both of those uncertainties, and driven  
12 by both fundamental ecological questions and applied needs (Botsford et al., 2001;

White et al., 2010), a large body of theory has developed to describe how connectivity and local demography interact to determine whether marine metapopulations persist (Burgess et al., 2014; Botsford et al., 2019). Testing this theory, however, has proven substantially more difficult.

For any population to persist, individuals must on average replace themselves during their lifetime. Assessing replacement must account for demographic processes across the life cycle, including how likely individuals are to survive to the next age or stage, their expected fecundity at each stage, the survival to recruitment of any offspring produced, and the distribution of offspring across space (Hastings and Botsford, 2006). A metapopulation can persist via two mechanisms: 1) at least one patch achieves replacement in isolation (self-persistence), or 2) multiple patches receive enough recruitment to achieve replacement through multi-generational loops of connectivity with other patches in the metapopulation (network persistence) (Hastings and Botsford, 2006; Burgess et al., 2014). Theory predicts that habitat patches that are large relative to the mean dispersal distance are likely to be self-persistent (White et al., 2010).

New ways of identifying individuals and determining their origins now allow better measurements of connectivity in marine populations (Almany et al., 2017; D'Aloia et al., 2013). Additionally, a better appreciation of the relevant theory has led to measurement of the demographic factors necessary to assess persistence in field metapopulations (Carson et al., 2011; Hameed et al., 2016; Johnson et al., 2018; Salles et al., 2015). To date, research has suggested that populations on isolated islands can be self-persistent, which might be expected given that they lack nearby populations

36 from which to receive larvae (Salles et al., 2015). In contrast, small habitat patches  
spread across a larger reef metapopulation appear to rely on input from surrounding  
and intervening patches for persistence (Johnson et al., 2018). However, isolated  
39 habitat patches are rare in the marine environment and intervening habitat patches  
are important contributors to metapopulation dynamics. Persistence has yet to be  
quantified in the field for a continuous marine metapopulation, such as all of the  
42 patches along a coastline.

Here, we further our understanding of metapopulation dynamics in a network  
of patches along a coastline through a study of yellowtail anemonefish (*Amphiprion*  
45 *clarkii*) in the Philippines. We assessed persistence for all patches of habitat within  
a metapopulation spread across 30 km of coastline. Based on seven years of data,  
we found that, despite containing multiple patches with large abundances that were  
48 stable over time, the metapopulation was not likely to be persistent without immi-  
gration from outside patches.

## Methods

### 51 Persistence theory and metrics

We considered four primary metrics to assess whether and how the anemonefish  
metapopulation was persistent: 1) lifetime recruit production (LRP) to assess whether  
54 the metapopulation had enough offspring that survived anywhere to achieve replace-  
ment, 2) self-persistence (SP) to assess whether any individual patch could persist  
in isolation without input from other patches, 3) network persistence ( $\lambda_c$ ) to assess

57 whether the metapopulation was persistent as a connected unit, and 4) local replacement (LR) to assess whether a sufficient number of recruits were retained anywhere within the metapopulation to achieve replacement, without explicitly estimating dispersal patterns within the metapopulation. We explain each metric below in detail.  
60 To represent the uncertainty in our estimates, we calculated each metric 1000 times, sampling each input parameter from a distribution representing the uncertainty in  
63 the empirical estimate (details in SI A.9). In our results, we show best estimates of each metric along with uncertainty bounds, defined as the middle 95% of the distribution of values calculated in this Monte Carlo procedure.

66 **Lifetime recruit production (LRP)**

$LRP_i$  is the expected number of recruits a recruit on patch  $i$  will produce in its lifetime,

$$LRP_i = LEP_i \times S_e, \quad (1)$$

69 where  $LEP_i$  (lifetime egg production) is the patch-specific number of eggs a recruit produces in its lifetime and  $S_e$  (egg-recruit survival) is the fraction of eggs that survive to become recruits (Fig. D.1).

72 If  $LRP \geq 1$ , individuals produced enough surviving offspring, before considering dispersal, to potentially achieve replacement. If  $LRP < 1$ , the population could not persist without input from outside patches. We considered all recruits produced by  
75 adults in our metapopulation to estimate  $LRP_i$ , regardless of where they settled.

### **Self-persistence (SP)**

SP<sub>i</sub> is the number of offspring a recruit produces that survive to become recruits and  
78 settle in the natal patch,

$$SP_i = LRP_i \times p_{i,i}, \quad (2)$$

where  $p_{i,i}$  is the probability of larval retention on patch  $i$ .

A patch  $i$  is self-persistent if SP<sub>i</sub> ≥ 1. If at least one patch is self-persistent, the  
81 metapopulation as a whole persists as well (Hastings and Botsford, 2006; Burgess  
et al., 2014).

### **Network persistence ( $\lambda_c$ )**

84 Network persistence is the largest real eigenvalue  $\lambda_C$  of the realized connectivity  
matrix  $C$ ,

$$C_{i,j} = LRP_i \times p_{i,j}, \quad (3)$$

created by multiplying lifetime recruit production (LRP<sub>i</sub>) by dispersal probabilities  
87 among pairs of patches ( $p_{i,j}$ ) (Burgess et al., 2014). The diagonal entries of  $C$   
are the self-persistence values for each patch (SP<sub>i</sub>).

Network persistence explicitly considers dispersal of individuals among patches  
90 in addition to the reproduction and survival at each patch and requires  $\lambda_C \geq 1$  for  
the network to persist without outside input (Hastings and Botsford, 2006; White

et al., 2010; Burgess et al., 2014).

<sup>93</sup> **Local replacement (LR)**

Local replacement (LR) is the number of recruits a recruit produces in its lifetime that return to settle within the focal metapopulation. LR is related to LRP, but in contrast, LRP also includes recruits that settle outside of the focal metapopulation.  
<sup>96</sup> LR is defined as

$$\text{LR} = \text{LEP}_* \times R_e, \quad (4)$$

where  $\text{LEP}_*$  is lifetime egg production averaged across patches and  $R_e$  is the proportion of eggs that survived and returned to recruit at the patches in our focal metapopulation (the 30 km section of coastline).  $R_e$  is a modification of egg-recruit survival ( $S_e$ ) that implicitly includes dispersal.  
<sup>99</sup>

<sup>102</sup> If  $LR \geq 1$ , enough offspring were locally retained to achieve replacement if they were evenly spread among patches, but the actual dispersal patterns among the metapopulation patches may still prevent replacement if the pattern of multigenerational replacement does not satisfy the Hastings and Botsford (2006) criterion. LR and  $\lambda_c$  both assess the ability of our patches to persist as an isolated group, but LR treats the network as one large homogenous patch while  $\lambda_c$  explicitly accounts for  
<sup>105</sup> the struture and connectivity among patches.  
<sup>108</sup>

## Study species

We focused on a tropical metapopulation of yellowtail anemonefish (*Amphiprion clarkii*, Fig. 2c). Yellowtail anemonefish have a mutualistic relationship with anemones that house small colonies of fish (Buston, 2003b; Fautin et al., 1992). Yellowtail anemonefish are protandrous hermaphrodites and maintain a size-structured hierarchy; within an anemone, the largest fish is the breeding female, the next largest is the breeding male, and any smaller fish are non-breeding juveniles. The fish move up in rank to become breeders only after the larger fish have died. In the tropical patch reef habitat of the Philippines, yellowtail anemonefish primarily spawn from November to May and lay clutches of benthic eggs that the parents protect and tend (Ochi, 1989; Holtswarth et al., 2017). Larvae hatch after about six days and spend 7-10 days in the water column before returning to reef habitat to settle in an anemone (Fautin et al., 1992).

Anemonefish are well-suited to metapopulation studies because dispersal only occurs during the larval phase and adults have limited movement on discrete habitat patches (anemones) (e.g., Buston and D'Aloia, 2013; Salles et al., 2015; Almany et al., 2017). Yellowtail anemonefish tend to behave more like other reef fishes, with wider-ranging territories and stronger swimming abilities (Hattori and Yanagisawa, 1991; Ochi, 1989) than the smaller *A. percula* commonly used in metapopulation studies (e.g., Buston et al., 2011; Salles et al., 2015).

<sup>129</sup> **Field data collection**

We focused on a set of nineteen reef patches spanning 30 km along the western coast of Leyte island facing the Camotes Sea in the Philippines (Fig. 2a). The habitat patches covered approximately 20% of the sampling region and consisted of rocky patches of coral reef separated by sand flats (Fig. 2a,b). To the north, the patches were isolated from nearby habitat with no substantial reef habitat for at least 20 km, a distance greater than the mean dispersal distance for this species (Pinsky et al., 2010). As such, we considered this to be a relatively isolated metapopulation. Located near a populated coastline, the region experiences anthropogenic effects including fishing, pollution, and runoff from agriculture and a nearby riverbed gravel mine, as well as reef-destroying storms like Haiyan and other typhoons in 2013.

From 2012-2018, we sampled fish and habitat at most patches each year (Table C.4). Divers using SCUBA and tethered to GPS readers swam the extent of each patch and visited anemones inhabited by yellowtail anemonefish. At each anemone, the divers caught fish 3.5 cm and larger, took a tissue sample, measured fork length, and noted tail color as an indicator of life stage (Moyer, 1976). Starting in 2015, fish 6.0 cm and larger were also tagged with a passive integrated transponder (PIT) tag unless already tagged. Divers also looked for eggs around each anemone and measured and photographed any clutches found. In total, we took fin clips from and genotyped 2406 fish and PIT-tagged 1929 fish across all years and patches combined, marking 3053 individual fish.

150 **Estimating demographic and dispersal parameters from empirical data**

### Parentage analysis and dispersal kernel

153 Over seven years of sampling, we genotyped 1729 potential parents and 791 juveniles at 1340 single nucleotide polymorphisms (SNPs) and found 71 parent-offspring matches (Catalano et al., in review). We used a distance-based generalized Gaussian  
156 dispersal kernel fit from the parent-offspring matches (Catalano et al., in review; Bode et al., 2018), where the relative probability of dispersal  $p(d)$  is a function of distance  $d$  in kilometers and parameters  $\theta$  and  $z = e^{K_d}$  that control the shape and  
159 scale of the kernel (Fig. 3a, Table C.1, uncertainty details in SI A.9). The dispersal kernel estimates the relative dispersal by distance for fish that have survived and recruited, so it does not separately estimate pre-settlement mortality. To find the probability of fish dispersing among our patches, we numerically integrated the dispersal kernel using the distance from the middle of the origin patch ( $i$ ) to the closest  
162 ( $d_1$ ) and farthest ( $d_2$ ) edges of the destination patch ( $j$ ), with distances calculated  
165 using the `geosphere` package in R (Hijmans, 2017):

$$p_{i,j} = \frac{z\theta}{2\Gamma(\frac{1}{\theta})} \int_{d_1}^{d_2} e^{-(zd)^{\theta}} dd. \quad (5)$$

## Growth and survival: mark-recapture analyses

Fish marked through geneotyping and PIT tags allowed us to estimate growth and  
168 survival through mark-recapture. In total, we had 3053 marked fish with size and  
stage data at each capture.

For growth, we used a von Bertalanffy growth curve:

$$\begin{aligned} L_{t+1} &= L_t + (L_\infty - L_t)[1 - e^{(-k)}] \\ &= e^{(-k)}L_t + L_\infty[1 - e^{(-k)}], \end{aligned} \tag{6}$$

171 where  $L_\infty$  is the asymptotic maximum size across the metapopulation and  $k$  is  
the growth rate. We estimated the parameters from the slope  $m$  and y-intercept  $b$   
of the relationship between the length at first capture  $L_t$  and the length at a later  
174 capture date  $L_{t+1}$  for fish recaptured a year later (within 345 to 385 days). The von  
Bertalanffy parameters are  $k = -\ln(m)$  and  $L_\infty = b(1 - m)$  (Hart and Chute, 2009)  
(Fig. 3b, Table C.1, uncertainty details in SI A.9).

177 We used the full set of marked fish to estimate annual survival  $\phi$  and probability  
of recapture  $p_r$  using the mark-recapture program MARK implemented in R through  
the package **RMark** (Laake, 2013). We fit several models with year, size, and patch  
180 effects on the probability of survival on a log-odds scale and selected the model with  
the lowest  $AIC_c$  (Fig. 3c, details in SI A.3, uncertainty details in SI A.9, and full list  
of models in Table C.3).

183 **Fecundity**

From a regression of eggs per clutch on female size while accounting for egg age (determined by the presence of eyed eggs), we found that fecundity increased with 186 size (eqn. A.1, see details in SI A.4). We only considered reproductive effort for female fish. For sex transition size  $L_f$ , we used the average size at which recaptured fish were first observed as female (Fig. 3d, uncertainty details in SI A.9).

189 **Lifetime egg production (LEP)**

We used an integral projection model (IPM) (Ellner et al., 2016) with size as the continuous structuring trait  $L$  to estimate lifetime egg production on each patch  $i$  192 ( $\text{LEP}_i$ ). We initialized the IPM with one recruit-sized individual (recruit defined in SI A.1) at the initial annual time step ( $t = 0$ ), then projected forward for 100 years. We used the size- and site-dependent survival (eqn. B.1) and growth (eqn. 6) 195 functions as the probability density functions in the kernel to project the individual into the next time step. The size distribution ( $v_L$ ) at each time step represents the probability that the individual has survived and grown into each of the possible size categories, ranging from a minimum of  $L_s = 0$  cm to a maximum of  $U_s = 15$  cm 198 divided into 100 equal size bins.

We then multiplied the size-distribution  $v_{L,t}$  at each time by the size-dependent 201 fecundity  $f_L$  (eqn. A.1) to get the total number of eggs produced at each time step. Integrating across time and size gave the total number of eggs one recruit produced in its lifetime (details in A.5, uncertainty details in SI A.9):

$$\text{LEP} = \int_{t=0}^{\infty} \int_{L=L_s}^{L=U_s} v_{L,t} f_L dL dt. \quad (7)$$

<sup>204</sup> We calculated LEP by patch ( $\text{LEP}_i$ ) and averaged across patches ( $\text{LEP}_*$ ) for a fish of recruit size. We also calculated LEP for a fish of parent size (6.0 cm) averaged across patches ( $\text{LEP}_p$ ), which is used below to estimate egg-recruit survival.

<sup>207</sup> **Accounting for density dependence**

We would ideally assess persistence when the population is at low abundance and not limited by density dependence; at high density the population growth rate will slow to zero. Density dependence is particularly clear in anemonefish. Juveniles will prevent others from settling such that each anemone can house only one recently settled anemonefish (Buston, 2003a). This density-dependent mortality reduces the apparent survival of new recruits from our field measurements. We accounted for this effect by scaling up our estimate of recruits (the numerator of eqn. 8, described next) by the proportional increase (DD) in unoccupied anemones if all of the anemones occupied by yellowtail anemonefish were unoccupied, where  $p_A$  is the proportion of anemones occupied by yellowtail anemonefish and  $p_U$  is the proportion of unoccupied anemones:  $\text{DD} = \frac{(p_U + p_A)}{p_U}$ . We present results with this density dependence modification in the main text and without the modification in the appendix (with subscript DD, Figs. D.9, D.10).

## Survival from egg to recruit ( $S_e$ )

We estimated survival from egg to recruit ( $S_e$ ) using parentage matches to find the number of surviving recruits produced by genotyped parents (similar to Johnson et al., 2018). However, the number of offspring we assigned back to parents ( $R_m$ ) is an underestimate of the offspring produced by genotyped parents because it is impossible to sample exhaustively. To account for unsampled offspring, we divided  $R_m$  by four factors (described below and with details in SI A.8 and diagram Fig. D.2), in addition to multiplying by DD as described above, then divided by the number of eggs produced by genotyped parents:

$$S_e = \frac{\frac{DDR_m}{P_h P_c P_d P_s}}{N_g \text{LEP}_p}, \quad (8)$$

where  $N_g$  was the number of genotyped parents and  $\text{LEP}_p$  was the expected lifetime egg production for a fish that has already survived to parent size  $p$  (=6.0cm).  $P_h$  was the cumulative proportion of habitat in our patches that we sampled over time (details in SI A.8),  $P_c$  was the probability of capturing a fish if we sampled its anemone (details in SI A.8),  $P_d$  was the proportion of the total dispersal kernel from each of our patches covered by our sampling region (details in SI A.8), and  $P_s$  was the proportion of suitable habitat in our sampling region (details in SI A.8).

To estimate the survival and retention of recruits back to our patches (needed for local replacement, LR, eqn. 4), we scaled only by  $P_h$  and  $P_c$ :

$$R_e = \frac{\frac{DDR_m}{P_h P_c}}{N_g \text{LEP}_p}. \quad (9)$$

## Estimated abundance over time

<sup>240</sup> We examined trends in abundance of breeding females at each patch over time ( $F_{i,t}$ ) to compare to our replacement-based persistence estimates. As with offspring, we scaled up the number of females caught ( $F_{c_{i,t}}$ ) at each patch  $i$  in each sampling year <sup>243</sup>  $t$  by the proportion of habitat sampled in that patch and year ( $P_{h_{i,t}}$ ) and by the probability of capturing a fish  $P_c$ :

$$F_{i,t} = \frac{F_{c_{i,t}}}{P_{h_{i,t}} P_c} \quad (10)$$

We fit a mixed effects model to estimate the number of fish in each year as a <sup>246</sup> Poisson-distributed variable  $\lambda_a$  with random effects by patch for both intercept and slope through time using the package `lme4` in R (Bates et al., 2015).

## Exploring alternative geographies and larval navigation

<sup>249</sup> To understand whether results would likely be similar in other geographies, we tested the sensitivity of metapopulation persistence to alternative patch widths and to the proportion of the region that is habitat. We varied the proportion of habitat and the <sup>252</sup> overall width of the region using 19 equally sized and spaced patches. We created connectivity matrices using the new distances between patches and otherwise used the original parameter values and uncertainty sets, using adult survival from the

255 patch with median survival (the Elementary School patch) for all patches.

We also tested sensitivity to the ability of larvae to navigate to habitat by adding up to a 1km buffer to the edges of the destination patches when integrating the dispersal kernel and adjusting the scaling parameter  $P_s$  (eqn. 8) to account for fewer larvae being lost between patches (details in SI A.7).

## Results

### 261 Demographic rates

From field data, mark-recapture, and parentage analyses, we estimated growth (Fig. 3b, SI B.3), fecundity (SI A.4), annual survival (Figs. 3c, D.5, SI B.4), lifetime egg production (Fig 4a, SI B.6), egg-recruit survival (Fig. D.13, SI B.7). Catalano et al. (in review) and the dispersal kernel (Fig. 3a, SI B.2). Details and estimated values are in Table C.1 and SI B. These demographic rates form the basis for assessing whether and how the metapopulation persists,

### Persistence metrics

Using our demographic and dispersal results, we estimated average lifetime recruit production (LRP) across patches to be 1.74 [0.94, 5.68] (Figs. 4b, D.12). Best estimates of  $LRP_i$  at individual patches ranged from 0 to 3.7 (Table C.5, Fig. D.8). Averaged across patches, 95% of LRP estimates were  $\geq 1$ , which means that individuals produced enough offspring to replace themselves. However, LRP does not tell us whether those offspring settled in locations that contributed to persistence.

Considering retention of larvae at individual patches, we did not find any patches  
276 with  $SP_i \geq 1$  (Fig. 5a), suggesting that no patch could persist in isolation. The Haina patch came closest to - but was still far from - self-persistence ( $SP_i = 0.044$  [0.005, 0.23]).

279 For network persistence, our estimate of  $\lambda_c$  was 0.18 [0.09, 0.63]. None of the uncertainty distribution of  $\lambda_c$  was  $\geq 1$  (Figs. 5c, D.14), suggesting network persistence for this metapopulation was therefore extremely unlikely if not impossible.  
282 Our estimate of local replacement (LR) was 0.20 [0.11, 0.65], also suggesting lack of independent persistence of our group of patches and very similar to our  $\lambda_c$  estimate. While both LR and  $\lambda_c$  provide information on the ability of our patches to persist  
285 as an isolated group, they differ in their assumption of the structure of the population. LR approximates the network of patches as a single well-mixed unit, while  $\lambda_c$  incorporates the spatial structure of the patches and multi-generation dynamics.  
288 Results without density dependence compensation also suggested lack of persistence (SI B.8).

## Abundance

291 Our estimated abundance of females over time had a positive trend for the average patch (slope = 1.08, Fig. 4a), suggesting a slight increase in population size through time. Most individual patches also showed a positive trend in female abundance  
294 through time (Figs. 4a, D.7s). Therefore, though the metapopulation did not exhibit network persistence, it also did not show signs of decline over the time scale of our study.

<sup>297</sup> **Alternative production and geographies**

We then examined what conditions would be needed for this metapopulation to reach persistence. With the existing patch configuration and dispersal kernel, the system  
<sup>300</sup> would need  $LRP \geq 8.9$  (a five-fold increase) to reach network persistence. In turn, this would require a five-fold increase of egg-recruit survival ( $S_e$ ) or  $LEP_*$  or an equivalent combination of increases across both. If we alternatively considered all  
<sup>303</sup> arriving recruits as offspring (not just those originating within the metapopulation),  $LRP$  would be 11.1, which would be sufficient for persistence. Similarly, our estimate of LR using all recruits arriving to the patches gave an estimate  $> 1$  (2.21),  
<sup>306</sup> also suggesting there was recruit-recruit replacement for the metapopulation when immigrants were included.

Another route to persistence would be with a different dispersal matrix or habitat density. If dispersal was such that the metapopulation retained all offspring produced, the study region would be persistent because  $LRP > 1$ . With the observed dispersal, however, retaining all recruits is difficult to achieve. The coastline  
<sup>312</sup> had a low fraction of habitat (20%) and would need to be increased to about 86% before enough offspring are retained that the point estimate of  $\lambda_c > 1$  (Fig. 6a). In contrast, widening the region while maintaining the same habitat density (20%) did  
<sup>315</sup> not achieve persistence (Fig. 6b) unless habitat density was also increased (Fig. 6c). As the region widens, the habitat density necessary for persistence decreases, down to 74% habitat at a region of 50 km. In contrast, allowing for larval navigation had  
<sup>318</sup> little impact on persistence estimates (Fig. 6d).

## Discussion

In this first assessment of demographic persistence of a coastal marine metapopulation,  
321 we did not find strong evidence for either self-persistence of an individual patch or network persistence of the entire 30 km area as an isolated region. This inability to persist as an isolated region does not mean that the metapopulation  
324 was declining, however. Both population trends and replacement of recruits with immigrants showed that population levels were stable or increasing slightly. Taken together, these metrics suggest that the region required input of immigrants to persist.  
327 Despite encompassing a distance substantially larger than mean dispersal, the coastline only persisted as part of a larger metapopulation.

Theory for predicting persistence within patchy habitats has suggested that we  
330 expect self-persistence when the mean dispersal distance is small relative to patch size and network persistence in groups of patches when dispersal distances are much larger than patch sizes and where the proportion of habitat in the landscape is about  
333 10-40% (depending on the particular species, population, and maximum reproductive rate, Botsford et al., 2019). Individual patches in the focal metapopulation were too small for self-persistence, but the 30 km region we sampled was about triple the mean  
336 dispersal distance of yellowtail anemonefish estimated from previous genetic work (8-9 km, Pinsky et al., 2010; Catalano et al., in review). Rather than a continuous patch, however, the region was only about 20% habitat. Low habitat may result at least  
339 in part from habitat declines over recent decades, based on interviews with fishers in the early 2000s (Jennifer Selgraeth, pers. comm.). Increasing the proportion of

coastline with habitat in sensitivity tests, however, suggested that even 40% habitat  
342 coverage would not be sufficient to achieve persistence and this metapopulation would  
require almost continuous habitat to persist. Similar to fish on small patches in the  
Caribbean (Johnson et al., 2018), this anemonefish metapopulation depends on the  
345 production and connectivity of outside patches. One possible path to persistence  
would be through nearby patches with higher egg production or survival. In such a  
case, even a small increase in area could create a persistent network. Deeper reefs,  
348 for example, are often healthier than shallower reefs (Cinner et al., 2016); LRP<sub>i</sub>  
is highest at our deepest patch, Tomakin Dako. In this system, offshore reefs at  
Cuatro Islas or the Camotes Islands, for example, with higher coral cover and less  
351 silt, could have higher anemonefish survival and contribute disproportionately to  
regional metapopulation persistence.

Our finding of a lack of isolated persistence differs markedly from persistence  
354 findings of other reef fish metapopulations. On reefs surrounding Kimbe Island,  
Salles et al. (2015) report self-persistence of individual anemonefish subpopulations  
in lagoons that were of similar size (approximately 100-500m long) to our individual  
357 patches, as well as network persistence of the 800m wide metapopulation around the  
island. This persistence finding is at a dramatically smaller scale than for our focal  
metapopulation in the Philippines. Additionally, Johnson et al. (2018) estimated that  
360 four reefs of a combined area of only 2.6 km<sup>2</sup> (four 65 ha patches) would be sufficient  
for network persistence of a damselfish metapopulation across multiple islands in  
the Bahamas. This area is roughly equivalent to a 26 km coastline section, which  
363 is shorter than our sampling region. To persist, these two offshore metapopulations

either had much higher retention of recruits or higher LRP than did our coastline patches.

366 Though lack of sufficient connectivity and retention is thought to inhibit network persistence in some systems (e.g., insufficient retention of offspring within reserves for eastern oysters (*Crassostrea virginica*) in North Carolina; Puckett and Eggleston, 2016), low production of surviving recruits seems the likelier explanation in the Philippines. Recruit production was lower in the Philippines than in the Kimbe Island populations, where Salles et al. (2020) estimated that an average individual produced 0.54 offspring over two years that recruited back to the natal population, more than twice our similar estimate of local replacement ( $LR = 0.20$ ), which considered lifetime rather than biennial production of locally-recruiting offspring. Lower production at our patches could be due to lower egg production, slower growth, or lower adult survival, all likely affected by habitat quality (e.g. Salles et al., 2020; Hayashi et al., 2019). Our study system was near a populated coastline and experienced anthropogenic effects, including pollution and silt, that can reduce demographic rates. Adult survival, for example, was lower at the two patches just downstream of a gravel mine (N. and S. Magbangon). Even at our higher-survival patches (38% annual survival for a 6 cm fish and 53% for a 10 cm fish at Tomakin Dako, for example), survival was lower than estimates from the populations at Kimbe Island (85% annual survival, Salles et al., 2015). Estimates of annual survival in other reef fish species are closer to the lower survival we found for yellowtail anemonefish than the higher survival of *A. percula* at Kimbe Island (approximately 30% annual survival for bluehead wrasse (*Thalassoma bifasciatum*) and bicolour damselfish (*Stegastes partitus*), respectively;

<sup>387</sup> Warner and Hughes, 1988; Figueira et al., 2008). Metapopulation studies in other reef fish (e.g., Figueira, 2009) and marine species more broadly (Carson et al., 2011) are highly sensitive to adult survival and other demographic parameters.

<sup>390</sup> Temporal variability in demographic or dispersal parameters on a time scale longer than our sampling could also enable persistence of our patches in isolation (similar to the storage effect, Warner and Chesson, 1985) rather than as part of a <sup>393</sup> larger metapopulation. Successful recruitment events on the decadal scale, for example, sustain rockfish populations on the west coast of the United States through the intervening weak recruitment years (e.g. Tolimieri and Levin, 2005). Our study could <sup>396</sup> have missed a particularly strong recruitment event driven by variable ocean connectivity (simulations suggest that 20 years are necessary to capture the full extent of ocean variability in the Coral Triangle region surrounding our patches; Thompson <sup>399</sup> et al., 2018). Strong recruitment would need to occur at least once a generation to maintain patch populations without switching to colonization and extinction dynamics, however, which we do not see. Our study likely spans the generation time <sup>402</sup> of a yellowtail anemonefish (roughly 5 years) so variable strong recruitment, while possible, is unlikely to sustain our populations.

<sup>405</sup> Understanding marine population persistence in the context of broader metapopulation theory requires reconciling replacement-based persistence analysis with classic colonization-extinction and source-sink dynamics (SALE et al., 2006). At the patch level, many marine metapopulations do not exhibit the colonization-extinction <sup>408</sup> dynamics (or do only on a decades to centuries timescale, Smedbol et al., 2002) that underpin our understanding of many terrestrial metapopulations (e.g, Hanski, 1998;

Moilanen et al., 1998) and instead consist of continuously-occupied patches connected  
411 by dispersal (Kritzer and Sale, 2006). Because dispersal is so widespread, patches  
in marine systems are not easily classified as sources or sinks in the classical fashion  
(Figueira and Crowder, 2006; White and Samhouri, 2011). For example, despite  
414 being unable to persist in isolation, our region is not technically a sink (Pulliam,  
1988) because  $LRP > 1$ . For metapopulations, lack of self-persistence can have two  
causes: reproduction does not balance mortality losses within a patch (a sink) or  
417 sufficient recruits are produced but not retained (as we found in the Philippines).  
Metapopulations likely lie on a continuum between extinction-colonization dynam-  
ics and exchange among populated patches (Kritzer and Sale, 2006) but the latter  
420 many be a more practical approach to characterizing dynamics for metapopulations  
in which exchange is frequent relative to organisms' generations times (Hastings and  
Botsford, 2006).

423 Density dependence also presents a sampling challenge. Persistence criteria (Hast-  
ings and Botsford, 2006; Burgess et al., 2014) ask whether a population at low abun-  
dance can grow and recover rather than going extinct. In real populations, however,  
426 it can be challenging to estimate density-independent demographic rates because  
density dependence is occurring in the population as it is sampled during dispersal  
(Nowicki and Vrabec, 2011) and reproduction (Roddenhouse et al., 2003). In anemone-  
fish, density dependence is likely most important immediately post-settlement, as it  
429 is for many species, including corals, trees, and butterflies (Vermeij and Sandin,  
2008; Harms et al., 2000; Nowicki et al., 2009). However, density dependence could  
432 continue to be important throughout life due to social hierarchies in anemonefish

colonies (Buston and Elith, 2011). Our calculations of self-persistence in this paper did not account for longer term post-settlement density dependence, which would be  
435 an interesting area of further research.

Understanding persistence is critical for the management of spatial populations, such as siting marine protected areas (Kaplan et al., 2009), assessing habitat fragmentation risks (Smith and Hellmann, 2002; Fahrig, 2001) and conserving species  
438 in the face of climate change (Coleman et al., 2017; Fuller et al., 2015). Though models and theory provide us with expectations, we are only recently beginning to  
441 be able to tackle these questions of persistence empirically in model systems such as anemonefish and other sedentary tropical reef fish (Salles et al., 2015; Johnson et al., 2018). With parentage analyses now being extended to temperate marine  
444 species (Baetscher et al., 2019) and a better understanding of how biophysical models compare to larval dispersal patterns (Bode et al., 2019), we are beginning to move beyond model species and investigate persistence in harvested and spatially-managed  
447 systems (Garavelli et al., 2018). Our study shows the importance of long-term sampling and careful consideration of the demographic and sampling processes that affect persistence calculations in order to determine persistence mechanisms and assess  
450 persistence state to understand marine population dynamics in empirical systems.

# Figures

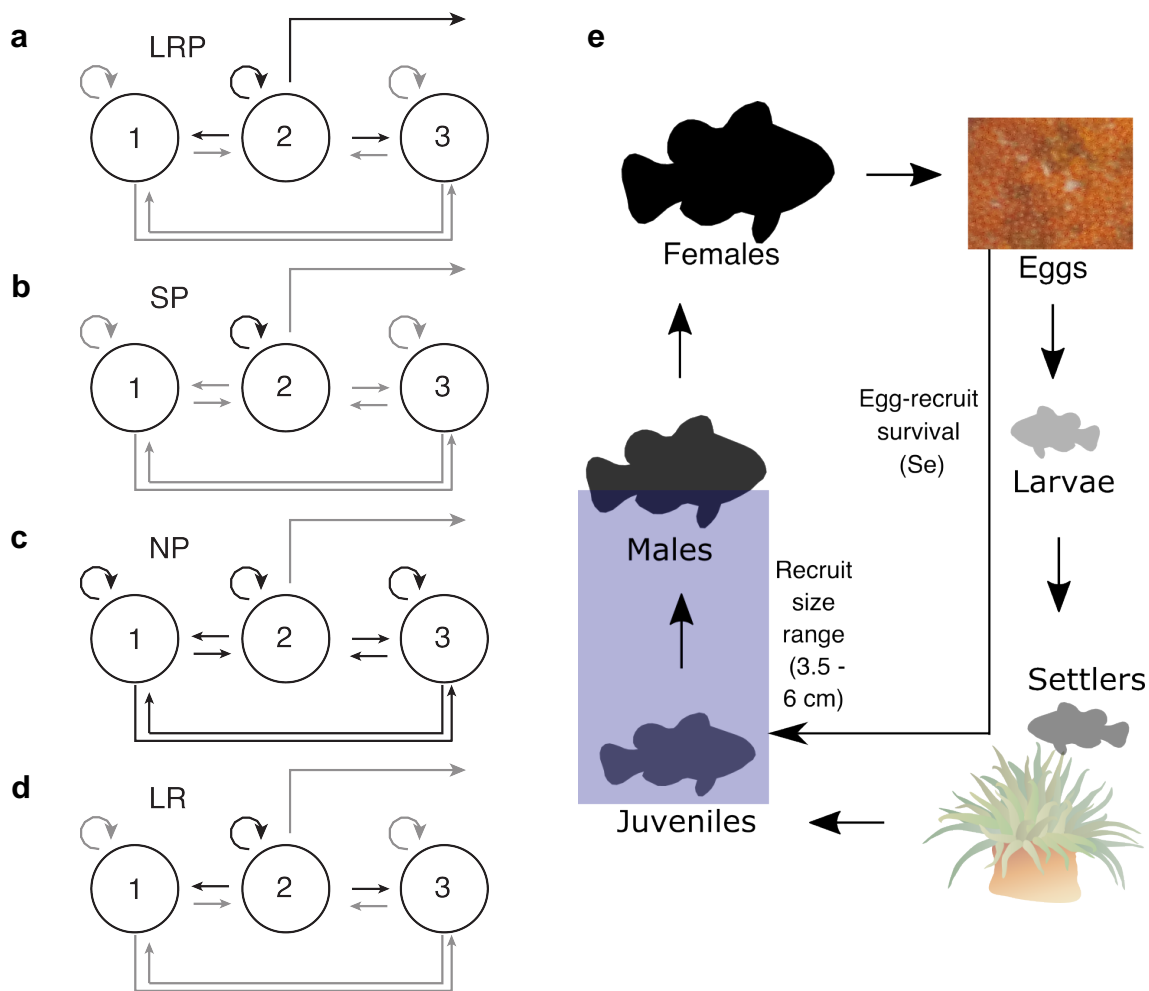


Figure 1: Schematics of the persistence metrics (a-d): a) lifetime recruit production (LRP, eqn. 1), b) self-persistence (SP, eqn. 2), c) network persistence ( $\lambda_c$ , first eigenvalue of eqn. 3), and d) local replacement (LR, eqn. 4). e) The life cycle of yellowtail anemonefish, including the range of sizes considered to be recruits (recruit definition in SI A.1).

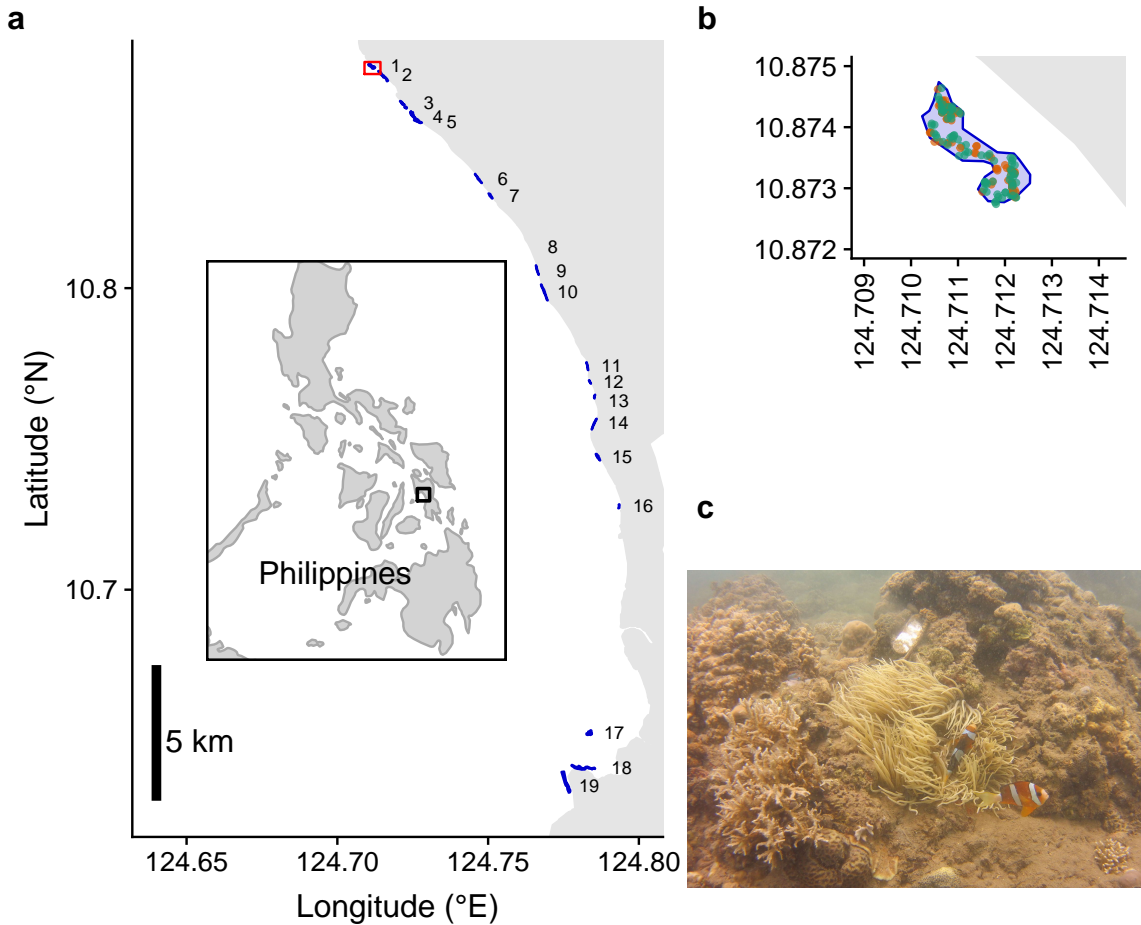


Figure 2: a) Map of the patches along the coast of Leyte in the Philippines. From north to south, the patches are: 1) Palanas, 2) Wangag, 3) North Magbangon, 4) South Magbangon, 5) Cabatoan, 6) Caridad Cemetery, 7) Caridad Proper, 8) Hicgop South, 9) Sitio Tugas, 10) Elementary School, 11) Sitio Lonas, 12) San Agustín, 13) Poroc San Flower, 14) Poroc Rose, 15) Visca, 16) Gabas, 17) Tomakin Dako, 18) Haina, and 19) Sitio Baybayon. b) Zoomed-in map of the northern-most patch, Palanas (red box on map), to show anemone arrangement. Anemones are colored as occupied by yellowtail anemonefish (green) or unoccupied by anemonefish (orange). c) An example anemone occupied by yellowtail anemonefish in a typical habitat. The metal anemone tag is visible just above the anemone on the rock.

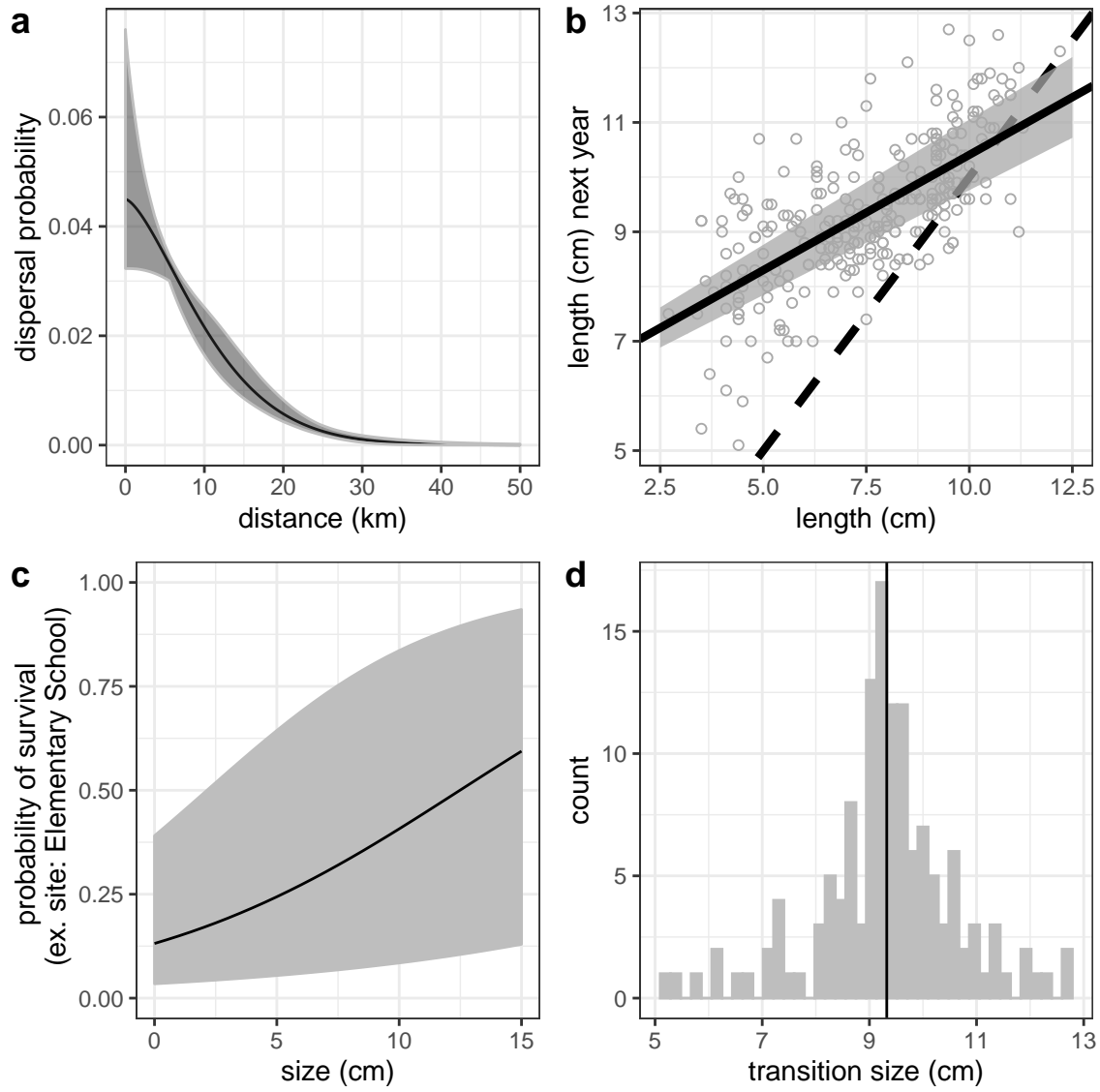


Figure 3: Estimates (solid black line) and uncertainty (grey) for a) dispersal (eqn. 5), b) growth (eqn. 6), including a dashed 1:1 line, c) post-recruit annual survival (eqn. B.1) at Elementary School as an example patch, and d) raw data of fish size at female transition ( $L_f$  in eqn. A.1).

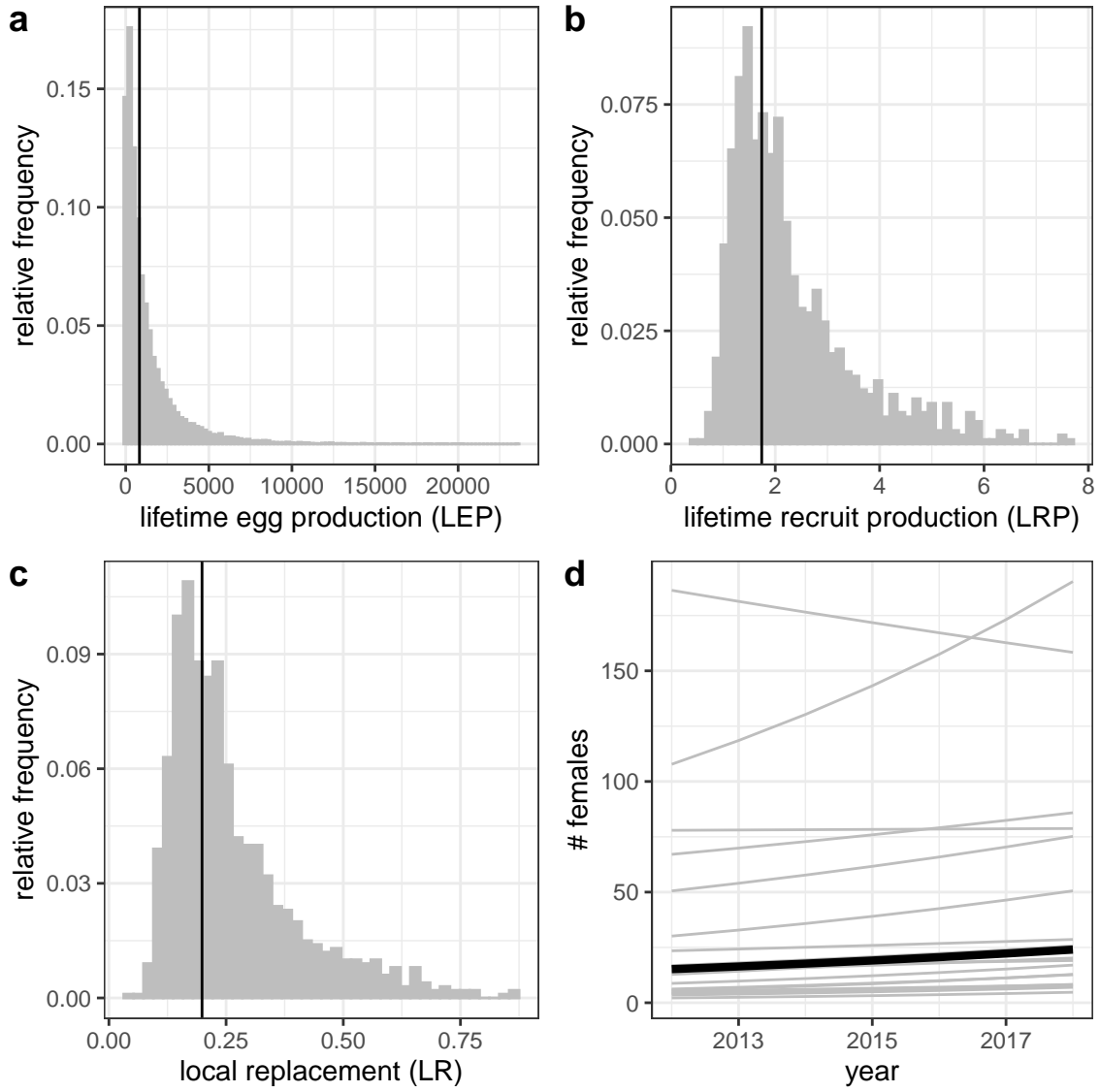


Figure 4: Estimates of a) individual-patch  $LEP_i$  (eqn. 7) for all patches with the point estimate averaged across patches ( $LEP_*$ , black line), b) average LRP across patches (eqn. 1), c) local replacement (eqn. 4), showing the point estimate (black solid line) and range of estimates considering uncertainty in the inputs (grey). Estimates of LRP and LR include compensation for density-dependent mortality in early life stages. d) Estimated abundance of females over time at each individual patch (grey lines) and for an average patch (black line).

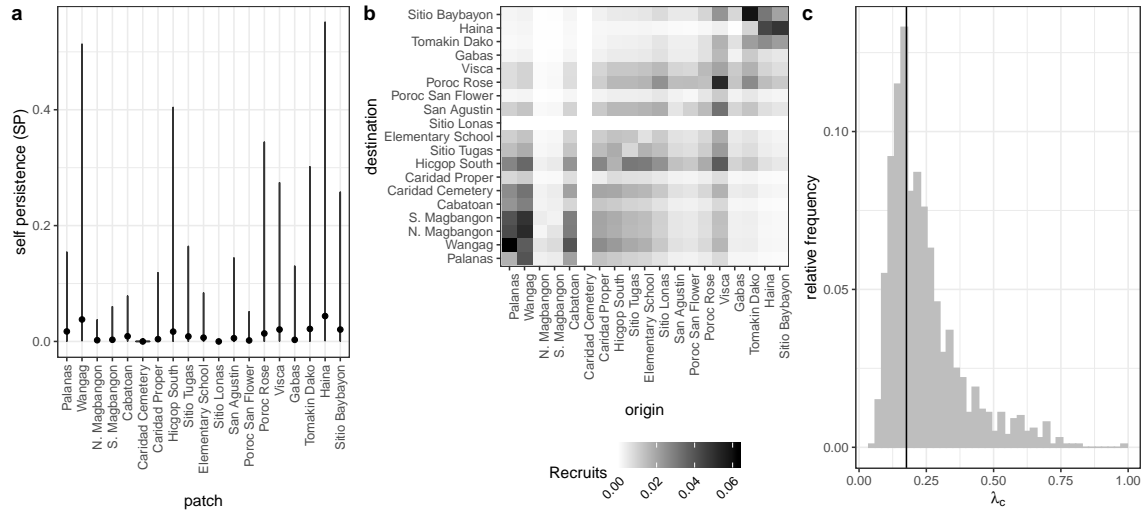


Figure 5: Values of a) self-persistence (SP, eqn. 2), b) realized connectivity among patches ( $C_{i,j}$ , eqn. 3), and c) network persistence ( $\lambda_c$ , first eigenvalue of eqn. 3). All estimates include compensation for density dependence in early life stages. For self-persistence (a) and network persistence (c), the best estimate is shown in black (point for (a), line for (c)) and the range of estimates considering uncertainty is shown in grey.

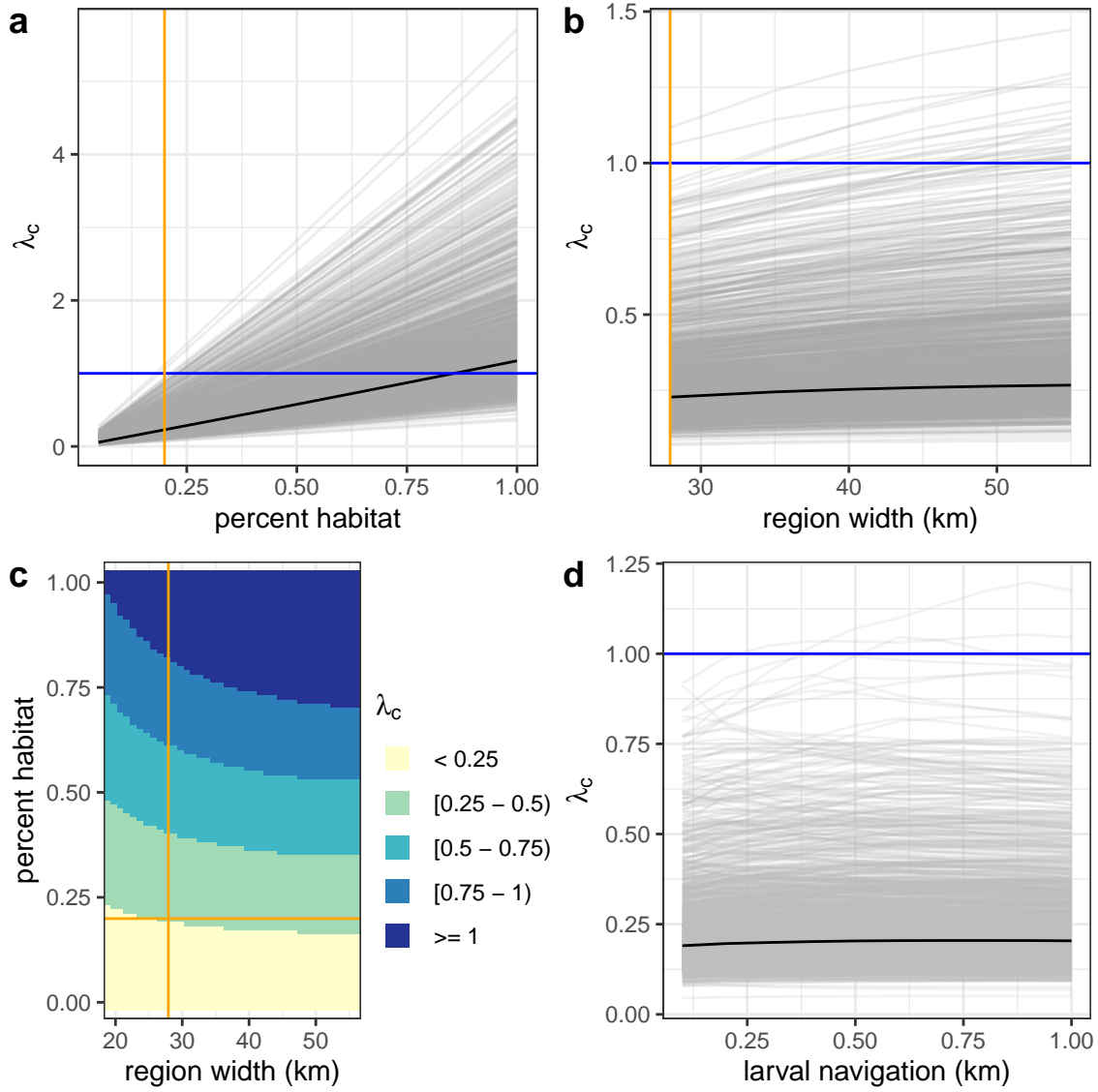


Figure 6: Sensitivity of network persistence ( $\lambda_c$ ) to a) the proportion of the sampling region that is habitat ( $P_s$ ), b) the width of a region with the same proportion habitat (20%), c) the region width and proportion habitat simultaneously, and d) larval navigation, where up to a 1 km buffer is added to the patch edges. The estimate is in black and each estimate with uncertainty is a grey line. The orange lines show the actual proportion habitat (20%) and region width (27 km) and the blue line shows the persistence threshold where  $\lambda_c = 1$ .

# Appendix

## <sup>453</sup> A Supplemental Methods

### A.1 Defining recruit and census stage

When assessing persistence, we must consider mortality and reproduction that occurs  
<sup>453</sup> across the entire life cycle to determine whether an individual is replacing itself with  
an individual that reaches the same life stage (Burgess et al., 2014). We defined a  
recruit to be a juvenile individual that has settled on the reef within the previous  
<sup>459</sup> year, which also encompasses the size of fish we were first able to sample (3.5-6.0 cm  
for parentage studies) (Figs. 1e, D.1). In theory, it does not matter how we defined  
recruit as long as we used that definition in our calculations of both egg-recruit  
<sup>462</sup> survival (eqn. 8) and LEP (eqn. 7). In our system, however, while it is straightforward  
to calculate LEP from any size, we did not have enough tagged recruits to reliably  
estimate survival from an egg to different recruit sizes. Instead, we chose the mean  
<sup>465</sup> size of offspring matched in the parentage study as our best estimate of the size  
of a recruit ( $\text{size}_{\text{recruit}} = 4.4 \text{ cm}$ ) and tested sensitivity to different recruit sizes by  
sampling from a uniform distribution over the sizes the recruit stage covers (3.5-6  
<sup>468</sup> cm, Table C.1, Figs. D.11-D.14).

### A.2 Self persistence (SP)

Our equation for SP (eqn. 2) is a modification of that used in Burgess et al. (2014),  
<sup>471</sup> which uses LEP to represent offspring produced and local retention (the number

of surviving recruits that disperse back to the natal patch divided by the number  
474 of eggs produced by the natal patch) to capture egg-recruit survival and dispersal  
combined: LEP x local retention  $\geq 1$ . We modify this to include egg-recruit survival  
in the offspring term instead, using LRP in place of LEP and probability of dispersal  
 $(p_{i,i})$  in place of local retention.

### 477 **A.3 Growth and survival**

To include size in the mark-recapture models for survival and recapture probability,  
we estimated sizes for fish in years when they were not recaptured. We used the  
480 growth model (eqn. 6) and the size recorded or estimated in the previous year to  
estimate the size of fish not recaptured in a particular year. Fish were not well-mixed  
at our patches, and divers needed to swim near an anemone to have a reasonable  
483 chance of capturing the fish on it. Therefore we also included a distance effect on  
recapture probability (eqn. B.2, Table C.3). We used diver GPS tracks to estimate  
the minimum distance between a diver and the anemone where the fish was first  
486 caught for each tagged fish in each sample year.

We compared the fit of the models using a modified version of the Akaike information criterion that reduces the potential for overfitting with small sample sizes  
489 (AICc) and selected the model with the lowest AICc value (Table C.3).

### **A.4 Fecundity**

We used a size-dependent fecundity relationship determined using photos of egg  
492 clutches and females from field sampling, where the number of eggs per clutch ( $E_c$ ) is

exponentially related to the length in cm of the female ( $L$ ) with size effect  $\beta_l = 2.388$ ,  
intercept  $b = 1.174$ , and egg age effect  $\beta_e = -0.608$  dependent on if the eggs were old  
495 enough to have visible eyes. For fish larger or equal to the transition to female size  
 $L_f$ , we multiplied the number of eyed eggs per clutch by the number of clutches per  
year  $c_e = 11.9$  (estimate from Holtswarth et al., 2017) to get total annual fecundity  
498  $f$  for a female of length  $L$ :

$$f(L) = \begin{cases} 0, & \text{if } L < L_f \\ c_e * e^{\beta_l \ln(L) + \beta_e [\text{eyed}] + b}, & L \geq L_f. \end{cases} \quad (\text{A.1})$$

## A.5 Lifetime egg production (LEP)

To compute LEP, we discretized time and size (in eqn. 7) and summed across the  
501 matrix. When entering the starting individual into the matrix, we used 0.1 as the  
standard deviation of size to spread out the starting individual across size bins. To  
account for differences in growth rates across fish, we used the size determined by  
504 the growth curve (eqn. 6) as the mean along with an estimate of spread ( $\text{size}_{sd}$ )  
when projecting the size distribution of the fish in the next year. To estimate  $\text{size}_{sd}$ ,  
we selected fish within 0.1 cm of the mean size at the first capture point for fish  
507 recaptured a year later (7.4-7.6 cm). We used the standard deviation of the sizes of  
those fish when they were recaptured one year later as  $\text{size}_{sd}$  (=1.45) (Table C.1).

LEP was estimated by patch ( $\text{LEP}_i$ ) because each patch has a different estimate  
510 of adult survival. We also present the average LEP across patches, noted as  $\text{LEP}_*$   
(Fig. 4b) and used to estimate average LRP and LR for the metapopulation (Fig.

4c, d).

513 To estimate egg-recruit survival ( $S_e$ ), we used the expected lifetime egg production for a fish that has already survived to reach parent size (6.0 cm) so  $L_s$  in eqn. 7 = 6.0, rather than 3.5. We used the average LEP for parent-sized fish across patches,  
516 noted as LEPp.

## A.6 Accounting for density dependence

In 2015 and 2017, we did a more thorough survey of anemones at sampled patches  
519 and noted anemones occupied by yellowtail anemonefish, occupied by other species of anemonefish, and unoccupied by anemonefish. We found the proportion of anemones occupied by yellowtail anemonefish ( $p_A$ ) and the proportion of anemones unoccupied  
522 by any anemonefish ( $p_U$ ) for all patches combined and averaged across the two sample years. We used these average proportions to estimate the proportional increase (DD) in unoccupied anemones if all anemones occupied by yellowtail anemonefish were  
525 unoccupied as described in the main text. We did not consider uncertainty in the effect of density dependence.

## A.7 Alternative geographies and larval navigation

### 528 Larval navigation

In our sensitivity test for larval navigation and swimming abilities, we added a buffer ranging from 0 - 1 km to the edges of the destination patches when determining  
531 probability of dispersal between patches. To avoid overlapping shadows of effective area of neighboring patches, we added no more than half the distance between two

adjacent patches to each patch. The buffers also changed the proportion of the  
534 sampling region that was habitat ( $P_h$ , see section in SI A.8), as we considered the  
buffer areas to be habitat as well, and affected the scaling of recruits (SI A.8) in  
egg-recruit survival (eqn. 8).

537 **A.8 Scaling up recruits**

To estimate the total number of offspring produced by genotyped parents that survived to recruitment, we scaled up the number of matched offspring caught during  
540 sampling ( $R_m$ ) to account for recruits our sampling could have missed (Fig. D.2). We scaled up by 1) the cumulative proportion of habitat we sampled at our patches over time ( $P_h$ ) to account for recruits at anemones we did not sample, 2) the probability  
543 of capturing a fish if we sampled its anemone ( $P_c$ ) to account for fish that escaped during sampling, 3) the proportion of the dispersal kernel from our patches covered within our sampling region ( $P_d$ ) to account for fish that dispersed outside  
546 of our sampling area (Fig. D.4, and 4) the proportion of our sampling region that was habitat ( $P_s$ ) to avoid counting mortality of fish dispersing to non-habitat within our region twice. The latter term is important because mortality from dispersing to  
549 non-habitat is both in the estimate of total recruits (numerator of eqn. 8) and in the integrated dispersal kernel (eqn. 5).

### Proportion of habitat sampled ( $P_h$ )

552 We used tagged anemones to estimate the proportion of habitat we sampled within our patches. We tagged each anemone that was home to yellowtail anemonefish with

a metal tag, which is relatively permanent and easy to re-sight (the anemone tag is  
555 visible above the anemone in Fig. 2c). We therefore considered the total number of  
metal-tagged anemones at a patch to be the habitat present. We used proportion of  
anemones rather than proportion of total patch area because anemones, and therefore  
558 habitat quality, were unevenly distributed across each patch; areas we did not visit  
typically had a lower anemone density than the areas we did sample.

To scale the number of sampled offspring from genotyped parents ( $R_m$ ) to account  
561 for areas of our patches we did not sample, we used the overall proportion habitat  
sampled across all patches and sampling years ( $P_h$ ). We summed the number of  
metal-tagged anemones we visited across all patches and years, then divided by the  
564 number of anemones we could have sampled (the sum of total metal-tagged anemones  
across all patches multiplied by the number of sampling years). We did not consider  
uncertainty in the proportion of habitat sampled.

#### 567 Probability of capturing a fish, from recapture dives ( $P_c$ )

We used the probability of capturing a fish to scale up the number of sampled  
offspring from genotyped parents ( $R_m$ ) to account for recruits we missed by failing  
570 to capture them. To estimate the probability of capturing a fish given that we  
sampled its anemone ( $P_c$ ), we used mark-recapture data from recapture dives done  
within a sampling season. During some of the sampling years, we intentionally  
573 re-sampled some locations within a few weeks of the original sampling dives. We  
assumed that the probability of recapturing a fish on a recapture dive was the same  
as capturing a fish on a sampling dive, essentially that there was no mortality in the

weeks between dives and that the fish did not alter their behavior towards divers.  
 For each recapture dive, we used GPS tracks of the divers to identify the anemones  
 covered in the recapture dive and the set of PIT-tagged fish encountered on those  
 anemones during the original sampling dives. We estimated the probability of capture  
 $P_c$  as the number of tagged fish re-caught during the capture dive  $m_2$  divided by the  
 total number of fish caught on the recapture dive  $n_2$ :  $P_c = \frac{m_2}{n_2}$ .

We used the mean  $P_c$  across all 14 recapture dives, covering 10 patches over three  
 sampling seasons (2016, 2017, 2018), as our best estimate. Uncertainty details are  
 in SI A.9.

### Proportion of dispersal kernel area sampled ( $P_d$ )

To account for recruits that dispersed outside our sampling region, we found the  
 proportion of the dispersal kernels from all parents that fell within our sampling  
 region (Fig. D.4). For each patch  $i$ , we found the area under the kernel ( $A_i$ ) from  
 the center of the patch to the north edge of the sampling area ( $d_{N,i}$ ) (northern-most  
 tagged anemone at Palanas, the northern-most patch) and from the center of the  
 patch to the south edge of the sampling area ( $d_{S,i}$ ) (southern-most tagged anemone  
 at Sitio Baybayon, the southern-most patch), then multiplied by the number of  
 genotyped parents at that patch ( $N_{g_i}$ ):

$$A_i = N_{g_i} \frac{z\theta}{2\gamma(\frac{1}{\theta})} \left( \int_0^{d_N} e^{-(zd)^{\theta}} dd + \int_0^{d_S} e^{-(zd)^{\theta}} dd \right). \quad (\text{A.2})$$

We added the areas together, then divided by the total number of genotyped

parents ( $N_g$ ) to get the proportion of the total dispersal kernel area covered by our sampling region ( $P_d$ ):

$$P_d = \frac{\sum_{i=1}^{19} A_i}{N_g}. \quad (\text{A.3})$$

597 We did not consider uncertainty in  $P_d$ .

### Proportion habitat in sampling area ( $P_s$ )

To avoid implicitly counting mortality due to larvae settling on non-habitat twice -  
600 once in scaling up our matched recruits (who settled on habitat) and once in integrating  
the dispersal kernel - we scaled the estimate of total recruits produced by parents  
on our patches by the proportion of our sampling region that was habitat ( $P_s$ ). We  
603 found  $P_s$  by summing the lengths of all the patches, which run approximately north-  
south, and dividing by the total north-south distance of our sampling region, giving  
 $P_s = 0.20$ . We assumed that larvae were unable to navigate to habitat if they dis-  
606 persed to an unsuitable area but relaxed that assumption in our sensitivity tests  
(SI A.7) because anemonefish larvae do likely have some ability both to sense good  
settlement areas by detecting host anemones (Elliott et al., 1995; Arvedlund et al.,  
609 1999) or conspecifics (e.g., Lecchini et al., 2005, for coral reef fish more broadly), and  
to swim in a particular direction (e.g., Bellwood and Fisher, 2001; Fisher, 2005).

## A.9 Characterizing uncertainty

### 612 Dispersal kernel

To account for uncertainty in the dispersal kernel, we used sets of the shape parameter  $\theta$  and the scale parameter  $K_d$  that represented the span of the 95% confidence interval 615 when  $K_d$  and  $\theta$  were estimated jointly (Table C.1, Fig. 3a, Catalano et al., in review). We randomly sampled pairs of  $\theta$  and  $K_d$  parameters from the distribution, weighted by the log-likelihood.

### 618 Growth

We used the first and second capture lengths for fish that were recaptured after a year (within 345 to 385 days) to estimate  $L_\infty$  and  $k$  (using eqn. 6). For fish recaptured 621 more than once, we randomly selected only one recapture period from each to use to estimate the von Bertalanffy parameters and repeated the random selection and estimate 1000 times. We found the mean estimates ( $L_\infty = 10.70$  cm,  $k = 0.864$ ) and 624 mean standard error of those fits, then sampled from within that range to generate a set of von Bertalanffy growth curves to use in our LEP calculations (Figs. 3b, D.3b, Table C.1).

### 627 Survival

We incorporated uncertainty in adult survival by sampling from within the 95% confidence limits for the patch-based survival estimates and size effect on survival 630 as estimated by the lowest AICc model from MARK (Table C.2, Fig. D.5). For

the simulations for the alternative geographies and larval navigation, we used the survival estimate and 95% range for the patch with median survival (Elementary School).  
633

### Size of transition to female ( $L_f$ )

To incorporate uncertainty in the size at which male fish transition to female ( $L_f$ ), we  
636 sampled with replacement directly from the sizes at which recaptured fish were first captured as female (5.2 cm - 12.7 cm) (Fig. 3d). Reproductive output is only counted once fish reach the female stage, so  $L_f$  affects fecundity (eqn. A.1) and therefore the  
639 fecundity kernel in calculating lifetime egg production ( $f_L$  in eqn. 7).

### Recruit size (size<sub>recruit</sub>)

We incorporated uncertainty in the size of a recruit (size<sub>recruit</sub>) by sampling from a  
642 uniform distribution across the ranges of possible sizes of recruits for the parentage analysis (3.5-6.0 cm) (Fig. D.3a). Recruit size enters into LEP as the starting size of the individual fish.

### Probability of capturing a fish ( $P_c$ )

To consider uncertainty in the probability of capturing a fish given that we sampled its anemone ( $P_c$ ), we represented the probability of capture as a beta distribution,  
648 using the mean  $\mu_{P_c}$  and variance  $V_{P_c}$  of the set of 14 values calculated from individual recapture dives to find the appropriate  $\alpha_{P_c}$  and  $\beta_{P_c}$  parameters, where

$$\alpha_{P_c} = \left( \frac{1 - \mu_{P_c}}{V_{P_c}} - \frac{1}{\mu_{P_c}} \right) \mu_{P_c}^2 \quad (\text{A.4})$$

$$\beta_{P_c} = \alpha_{\mu_{P_c}} \times \frac{1}{\mu_{P_c} - 1}. \quad (\text{A.5})$$

The mean of the individual capture probability values was  $\mu_{P_c} = 0.56$ , with  
 651 variance  $V_{P_c} = 0.069$ , giving beta distribution parameters  $\alpha_{P_c} = 1.44$  and  $\beta_{P_c} = 1.13$ .  
 We sampled 1000 values from the beta distribution, then truncated the sample to  
 include only values larger or equal to the lowest value of  $P_c$  estimated from an  
 654 individual dive (0.20), to avoid unrealistically low values randomly sampled from the  
 distribution. We then sampled with replacement from the truncated set to get a  
 vector of 1000 values (Fig. D.3c).  $P_c$  is one of the scaling factors in the estimate of  
 657 egg-recruit survival (eqn. 8), accounting for recruits we missed by failing to capture  
 them.

### Lifetime Egg Production (LEP)

660 Uncertainty in lifetime egg production enters through adult survival (SI A.9), growth  
 (SI A.9), and the size of a recruit (SI A.9), all of which affect the size distribution  $v_L$   
 in eqn. 7. Additionally, uncertainty in the size of transition to female ( $L_f$ , SI A.9)  
 663 affects the fecundity kernel  $f_L$  in eqn. 7. We show the contribution of uncertainty of  
 each input in Fig. D.11.

### Egg-recruit survival ( $S_e$ )

In estimating egg-recruit survival ( $S_e$ ), we considered uncertainty in the number of offspring assigned to parents ( $R_m$ ) and in the probability of capturing a fish ( $P_c$ ). For offspring assigned to parents, we generated a set of values for the number of assigned offspring using a random binomial, with the number of genotyped offspring (791) as the number of trials and the assignment rate from the parentage analysis (0.090) as the probability of success on each trial (Catalano et al., in review), (Fig. D.3d). Uncertainty in probability of capture  $P_c$  is described in SI A.9. We show the contribution of uncertainty of each input in Fig. D.13.

## B Supplemental Results

### 675 B.1 Parentage

From the genetic work and parentage analysis done in Catalano et al. (in review), we genotyped 1729 potential parents, genotyped 791 potential offspring (recruits), and  
678 matched 71 offspring to parents, with an assignment rate of 9%. In estimates with uncertainty, the middle 95% distribution of matched offspring was 55 to 87 (Fig. D.3d, Table C.1).

681 The combined number of potential parents and potential offspring is higher than the number of genotyped fish because some fish are included as both a potential offspring and a potential parent (in different years).

### 684 B.2 Dispersal kernel

We used the dispersal kernel estimated for all years together in Catalano et al. (in review) (eqn. 5), with  $K_d = -2.51$  and  $\theta = 1.49$ . Using the 95% confidence surface  
687 when  $K_d$  and  $\theta$  were estimated jointly to incorporate uncertainty (SI A.9),  $K_d$  ranged from -2.86 to -1.82 and  $\theta$  from 0.87 to 2.46 (Fig. 3a, Table C.1).

### B.3 Growth

690 From the mark-recapture analysis of tagged and genotyped fish, we estimated mean values of  $L_\infty = 10.70$  cm with uncertainty bounds 9.81-11.65 and  $k = 0.864$  with uncertainty bounds 0.80-0.91 for the von Bertalanffy growth curve parameters (eqn.  
693 6, Fig. 3b, Table C.1).

## B.4 Survival

The best model for post-recruitment annual survival  $\phi$  on a log-odds scale had a  
696 positive size effect ( $b_a = 0.15 \pm 0.029$  SE) with intercepts  $b_{\phi_i}$  varying by patch (eqn.  
B.1, Fig. D.5, Table C.2):

$$\log\left(\frac{\phi}{1 - \phi}\right) = b_{\phi_i} + b_a \text{size}. \quad (\text{B.1})$$

The accompanying best model for recapture probability  $p_r$  on a log-odds scale  
699 had a negative effect of size ( $b_1 = -0.16 \pm 0.09$  SE) and a negative effect of diver  
distance from anemone ( $b_2 = -0.15 \pm 0.02$  SE), with intercept  $b_{p_r} = 2.14 \pm 0.87$  SE  
(eqn. B.2, Fig. D.6):

$$\log\left(\frac{p_r}{1 - p_r}\right) = b_{p_r} + b_1 \text{size} + b_2 d. \quad (\text{B.2})$$

702 This suggests divers were less likely to recapture larger fish, which are stronger  
swimmers and more likely to flee when divers approach, and those at anemones far  
from areas sampled.

## 705 B.5 Scaling factors

The proportion of habitat at patches sampled over time ( $P_h$ ) was 0.41, the proportion  
708 of the region that was habitat ( $P_s$ ) was 0.20, the proportion of the dispersal kernel  
that was within the sampling region ( $P_d$ ) was 0.57, and the probability of capturing  
a fish given that its anemone was sampled ( $P_c$ ) was 0.56 [0.22, 0.97] (Fig. D.3c, Table

C.1).

## 711 **B.6 Lifetime egg production (LEP)**

We calculated an average value of LEP ( $LEP_*$ ) across patches of 827 [227, 2919] eggs (Fig. 4b), with best estimate values at individual patches that ranged from 0 to 1760 eggs (Table C.5). Uncertainty in adult survival had the largest effect on LEP (Fig. D.11), which corresponds to longer-surviving individuals having more opportunities to reproduce at larger sizes.

## 717 **B.7 Egg-recruit survival ( $S_e$ )**

We estimated egg-recruit survival  $S_e$  to be  $0.002 [5 \times 10^{-4}, 0.01]$  when we accounted for density dependence in our data. Uncertainty in the size of transition to breeding female  $L_f$  had the largest effect on egg-recruit survival (Fig. D.13); the larger the transition size to female, the fewer tagged eggs we estimated were produced by our genotyped parents and the higher the estimate of egg-recruit survival. This differs from our finding above that adult survival had the largest effect on LEP because the starting size of the individual considered is lower when we estimate LEP for a recruit (4.4 cm, 3.5-6.0cm range) than for a parent (6.0cm). Fish considered parents in our parentage analysis have already survived one or more years since recruiting so the transition to breeding female plays a larger role in the number of eggs they are likely to produce than for fish who have just recruited.

729 **B.8 Persistence metrics without compensation for density dependence**

Estimating persistence metrics without compensating for density dependence in our data (subscript DD) gave us an understanding of whether individuals at our patches were able to replace themselves and whether our patches would persist in isolation at the current abundance levels, rather than at low abundance. Without compensation for early life density dependence, all of our metrics showed that the set of patches we sampled was less likely to persist as an isolated network than the metrics for low abundance. We estimated egg-recruit survival ( $S_{e_{DD}}$ ) to be 0.001 [ $3 \times 10^{-4}$ , 0.005] and average lifetime recruit production across patches ( $LRP_{DD}$ ) to be 0.96 [0.52, 3.14], with 57% of  $LRP_{DD}$  estimates  $\geq 1$  (Fig. D.9a). Our estimate of local replacement ( $LR_{DD}$ ), which estimates replacement for recruits from our patches returning to our patches implicitly including dispersal, was 0.11 [0.06, 0.36] (Fig. D.9b).

When we calculated LR using all arriving recruits to our patches, however, rather than just those originating there, the best estimate was  $> 1$  (1.22), suggesting that there was recruit-recruit replacement at our patches when we included immigrant recruits, even at current population levels when density dependence was present.

We did not find any patches with a best estimate of  $SP_{DD} \geq 1$  or with uncertainty bounds that reached or exceeded 1 (Figs. D.10a). Our best estimate of the dominant eigenvalue of the realized connectivity matrix  $\lambda_{c_{DD}}$  was 0.10 [0.05, 0.35] with 0% of estimates where  $\lambda_{c_{DD}} \geq 1$  (Fig. D.10c).

750 C Supplemental Tables

Table C.1: Summary of parameter symbols, definitions, and values, including sections and equations where each are described in detail.

Parameter	Description	Best estimate [uncertainty bounds]	Uncertainty origin	Details	Notes
<i>Dispersal and demographics</i>					
$K_d$	scale parameter in dispersal kernel	-2.51 [-2.86, -1.82]	drawn from joint 95% confidence limits with $\theta$ , weighted by log-likelihood	eqn. 5, SI A.9, B.2	estimated in Cata-lano et al. (in re-view) using methods in Bode et al. (2018)
$\theta$	shape parameter in dispersal kernel	1.49 [0.87, 2.46]	drawn from joint 95% confidence limits with $K_d$ , weighted by log-likelihood	eqn. 5, SI A.9, B.2	estimated in Cata-lano et al. (in re-view) using methods in Bode et al. (2018)
$L_\infty$	average asymptotic size (cm) in von Bertalanffy growth curve	10.7 cm [9.8, 11.6]	growth curve estimated with different pairs of fish	eqn. 6, SI A.3, A.9, B.3	
$k$	growth coefficient in von Bertalanffy growth curve	0.864 [0.795, 0.938]	growth curve estimated with different pairs of fish	eqn. 6, SI A.3, A.9, B.3	
size <sub>recruit</sub>	size of a recruit	4.4 cm [3.5-6.0]	sampled from a uniform distribution of range of offspring sizes for parentage analyses	SI A.1, A.9	used as starting size of fish in calculation of LEP (eqn. 7)

$b$	intercept at 0 cm for size-fecundity relationship	1.174 eggs	no uncertainty	eqn. A.1, SI A.4	
$\beta_l$	size effect for size-fecundity relationship	2.388 $\frac{\text{eggs}}{\text{cm}}$	no uncertainty	eqn. A.1, SI A.4	
$\beta_e$	egg age effect in fecundity	-0.608	no uncertainty	eqn. A.1, SI A.4	egg age was determined by the presence of visible eyes (eyed vs. non-eyed)
$c_e$	number of egg clutches per year	11.9	no uncertainty	eqn. A.1, SI A.4	estimate from Holtswarth et al. (2017)
$\text{size}_{\text{sd}}$	spread in sizes of fish one year later	1.45	no uncertainty	used in estimating LEP, SI A.5	estimated from recapture data
parent size	size of fish used to estimate LEP for parents (LEPp)	6.0 cm	no uncertainty	SI A.5	used in estimating egg-recruit survival ( $S_e$ , eqn. 8)
$R_m$	number of offspring matched to genotyped parents	71 [55, 87]	random binomial for each genotyped offspring using the assignment rate from the parentage analysis (9%)	SI A.9	used in calculating egg-recruit survival ( $S_e$ , eqn. 8)

genotyped offspring	number of recruits genotyped	791	no uncertainty	SI B.1	used to find mean recruit size ( $\text{size}_{\text{recruit}}$ ), estimate metrics with immigrants included
$N_g$	potential parents genotyped	1729	no uncertainty	SI B.1	used to find proportion of dispersal kernel area sampled ( $P_d$ , SI A.8)
$L_f$	size of transition to female	9.3 cm [5.2, 12.7]	sampled with replacement from transition sizes for recaptured fish	eqn. A.1, SI A.9	used to find fecundity (eqn. A.1)
$b_{\phi,ES}$	intercept at size = 0cm for survival at Elementary School patch	-1.88 [-3.33, -0.44]	sampled from within 95% confidence limits from MARK estimates	eqn. B.1, SI A.3, A.9, B.4	patch with median survival
$b_a$	size effect for survival	0.15 [0.10, 0.21]	sampled from within 95% confidence limits from MARK estimates	eqn. B.1, SI A.3, A.9, B.4	

*Scaling factors*

ξ	DD	proportional increase in unoccupied anemones to account for density-dependence at settlement	1.18	no uncertainty	section "Accounting for density-dependence", SI A.6	used to scale recruits for egg-recruit survival ( $S_e$ , eqn. 8)
	$p_A$	proportion anemones occupied by yellow-tail anemonefish	0.37	no uncertainty	SI A.6	
	$p_U$	proportion anemones unoccupied by anemonefish	0.46	no uncertainty	SI A.6	
	$P_h$	cumulative proportion of habitat in patches sampled	0.41	no uncertainty	SI A.8	used to scale recruits for egg-recruit survival ( $S_e$ , eqn. 8)
	$P_s$	proportion of region that was habitat	0.20	no uncertainty	SI A.8	used to scale recruits for egg-recruit survival ( $S_e$ , eqn. 8)
	$P_d$	proportion dispersal kernel area in sampling region	0.57	no uncertainty	SI A.8	used to scale recruits for egg-recruit survival ( $S_e$ , eqn. 8)
	$P_c$	probability of capturing a fish	0.56	sampled from a beta distribution	SI A.8, A.9	used to scale recruits for egg-recruit survival ( $S_e$ , eqn. 8)



Table C.2: Table with patch-specific survival ( $\phi_i$ ) values on a log-odds scale (used in eqn. B.1), where the intercept is for adult survival for a fish of size 0 cm. The intercept for each patch is the intercept for Cabatoan plus the additional intercept value for that patch, shown in the table.

Patch	Intercept	Standard error	Confidence limits	Notes
Cabatoan	-1.78	0.33	-2.42 to -1.14	
Caridad Cemetery	-19.66	0.00	-19.66 to -19.66	addition to Cabatoan intercept
Elementary School	-0.11	0.41	-0.92 to 0.69	addition to Cabatoan intercept
Gabas	-0.42	0.58	-1.55 to 0.72	addition to Cabatoan intercept
Haina	0.12	0.35	-0.57 to 0.81	addition to Cabatoan intercept
Higcop South	-0.06	0.46	-0.96 to 0.84	addition to Cabatoan intercept
N. Magbangon	-1.31	0.38	-2.05 to -0.57	addition to Cabatoan intercept
Palanas	0.24	0.26	-0.26 to 0.75	addition to Cabatoan intercept
Poroc Rose	-0.19	0.44	-1.05 to 0.68	addition to Cabatoan intercept
Poroc San Flower	-0.52	0.48	-1.45 to 0.42	addition to Cabatoan intercept
San Agustin	-0.47	0.50	-1.45 to 0.42	addition to Cabatoan intercept
Sitio Baybayon	0.02	0.26	-0.49 to 0.52	addition to Cabatoan intercept
S. Magbangon	-1.08	0.48	-2.02 to -0.14	addition to Cabatoan intercept
Tomakin Dako	0.39	0.33	-0.25 to 1.03	addition to Cabatoan intercept
Visca	0.33	0.35	-0.36 to 1.01	addition to Cabatoan intercept
Wangag	0.35	0.25	-0.15 to 0.85	addition to Cabatoan intercept

Table C.3: Table showing the set of models considered in MARK for survival ( $\phi$ , from eqn. B.1) and recapture probability ( $p_r$ , from eqn. B.2), including effects of fish size ( $L$ ), minimum distance from diver to the anemone where the fish was first caught during surveys ( $D$ ), year ( $t$ ), and patch ( $i$ ), and their relative AICc scores.

<b>Model</b>	<b>Model description</b>	<b>AICc</b>	<b>dAICc</b>
$\phi \sim L + i, p_r \sim L + D$	survival size+patch, recapture size+distance	3104.1	0
$\phi \sim i, p_r \sim L + D$	survival patch, recapture size+distance	3127.2	-23.1
$\phi \sim i, p_r \sim D$	survival patch, recapture distance	3127.2	-23.1
$\phi \sim L, p_r \sim L + D$	survival size, recapture size+distance	3139.9	-35.8
$\phi \sim L, p_r \sim D$	survival size, recapture distance	3141.6	-37.5
$\phi, p_r \sim L + D$	survival constant, recapture size+distance	3168.4	-64.3
$\phi, p_r \sim D$	survival constant, recapture distance	3169.3	-65.2
$\phi \sim t, p_r$	survival time, recapture constant	3243.9	-139.8
$\phi \sim i, p_r$	survival patch, recapture constant	3254.4	-150.3
$\phi, p_r \sim t$	survival constant, recapture time	3274.0	-169.9
$\phi \sim L, p_r \sim L$	survival size, recapture size	3345.1	-241.0
$\phi, p_r$	survival constant, recapture constant	3382.7	-278.6

Table C.4: Table showing the percent of anemones surveyed at each patch, ordered from north to south, in each sampling year.

		% Habitat surveyed						
Patch	# Total anems	2012	2013	2014	2015	2016	2017	2018
Palanas	138	29	57	48	61	85	86	86
Wangag	291	18	33	42	35	27	49	69
N. Magbangon	105	5	12	40	63	64	0	5
S. Magbangon	34	41	56	32	0	65	0	71
Cabatoan	26	42	58	58	65	73	0	62
Caridad Cemetery	4	0	75	50	0	50	50	50
Caridad Proper	4	0	100	0	0	0	0	0
Hicgop South	18	0	67	28	28	56	83	78
Sitio Tugas	8	0	100	0	0	0	0	0
Elementary School	7	0	100	43	100	100	86	100
Sitio Lonas	1	100	100	0	0	0	0	0
San Agustin	18	89	61	72	61	100	89	72
Poroc San Flower	11	100	82	73	73	55	82	64
Poroc Rose	13	100	100	69	31	23	69	69
Visca	13	100	100	23	38	62	85	62
Gabas	9	0	0	0	44	44	67	0
Tomakin Dako	48	0	25	23	38	35	60	69
Haina	104	0	6	13	13	10	56	80
Sitio Baybayon	259	0	14	30	34	30	41	81
Overall	1111	16	32	36	39	42	48	67

Table C.5: Table showing patch-specific estimates of lifetime egg production ( $LEP_i$ ), lifetime recruit production ( $LRP_i$ ), and self persistence ( $SP_i$ )

Patch	$LEP_i$	$LRP_i$	$SP_i$
Palanas	1383	2.91	0.017
Wangag	1642	3.45	0.040
N. Magbangon	133	0.28	0.002
S. Magbangon	183	0.39	0.003
Cabatoan	933	1.96	0.009
Caridad Cemetery	0	0	0
Caridad Proper	781	1.64	0.004
Hicop South	848	1.78	0.017
Sitio Tugas	781	1.64	0.003
Elementary School	781	1.64	0.007
Sitio Lonas	781	1.64	0
San Agustin	445	0.92	0.006
Poroc San Flower	415	0.87	0.002
Poroc Rose	694	1.46	0.014
Visca	1586	3.34	0.021
Gabas	483	1.02	0.003
Tomakin Dako	1760	3.70	0.022
Haina	1130	2.38	0.044
Sitio Baybayon	959	2.02	0.021

## D Supplemental Figures

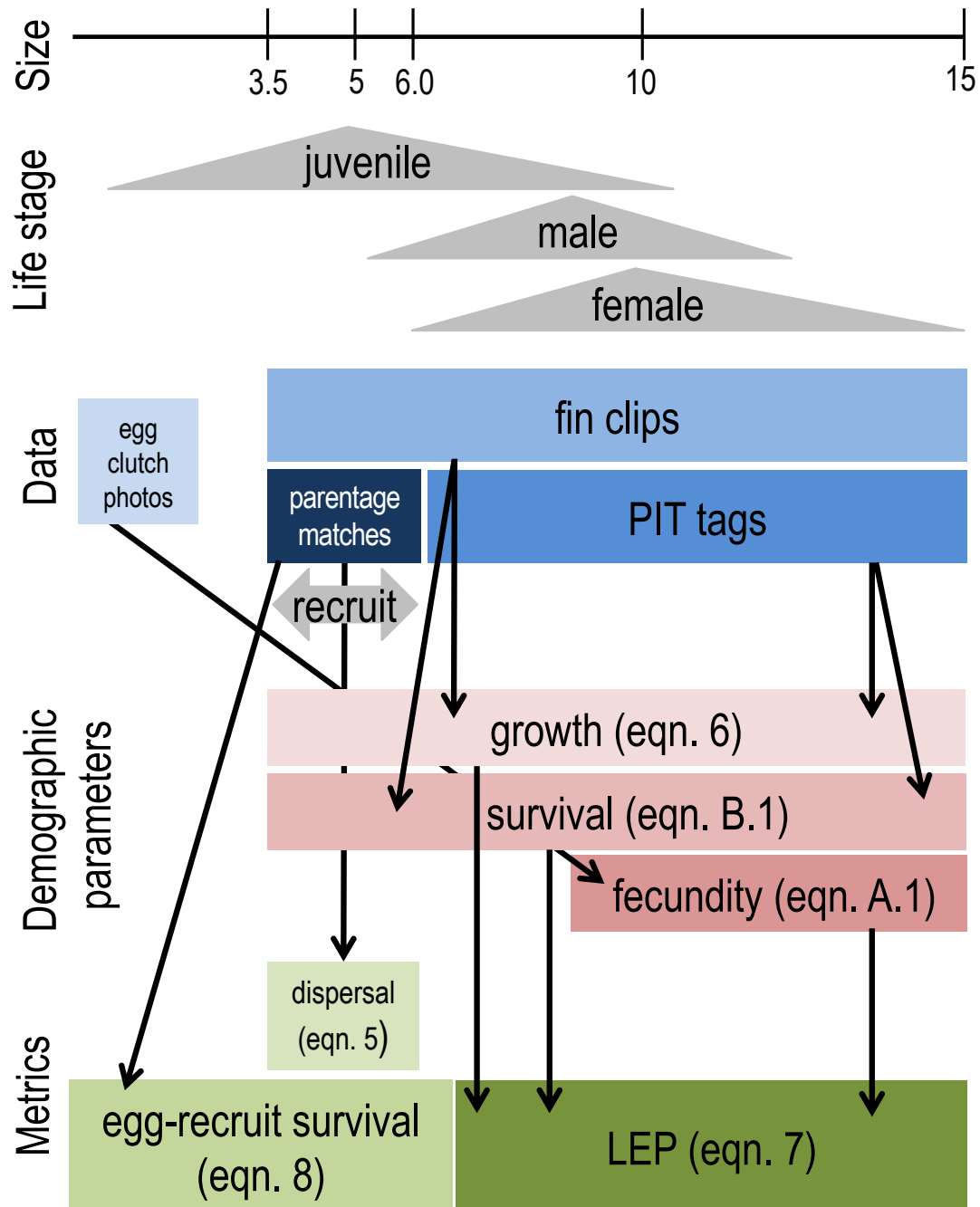


Figure D.1: The data collected for fish at each life stage and how they match to the equations and metrics estimated. We considered recruits to be offspring in their first year of settlement, represented by the 3.5–6.0 cm range (SI A.1).

## How could we have missed potential recruits originating from our patches?

- 1) Failed to catch recruit when sampling ( $P_c$ )
- 2) Missed sampling some habitat areas within our patches ( $P_h$ )
- 3) Recruit dispersed outside our study region ( $P_d$ )
- 4) Recruit dispersed to non-habitat within our region ( $P_s$ )
- 5) Recruit died due to density-dependent competition with other settlers (DD)

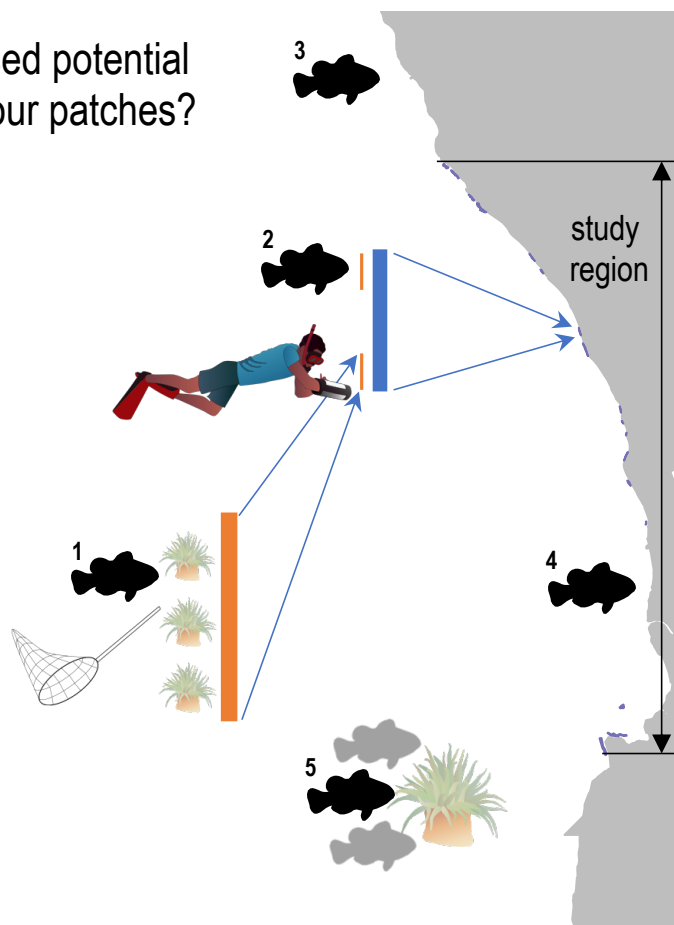


Figure D.2: Schematic of five ways we could have missed recruits while sampling. We used these factors to scale up our raw estimate of recruits from matched offspring (SI A.8).

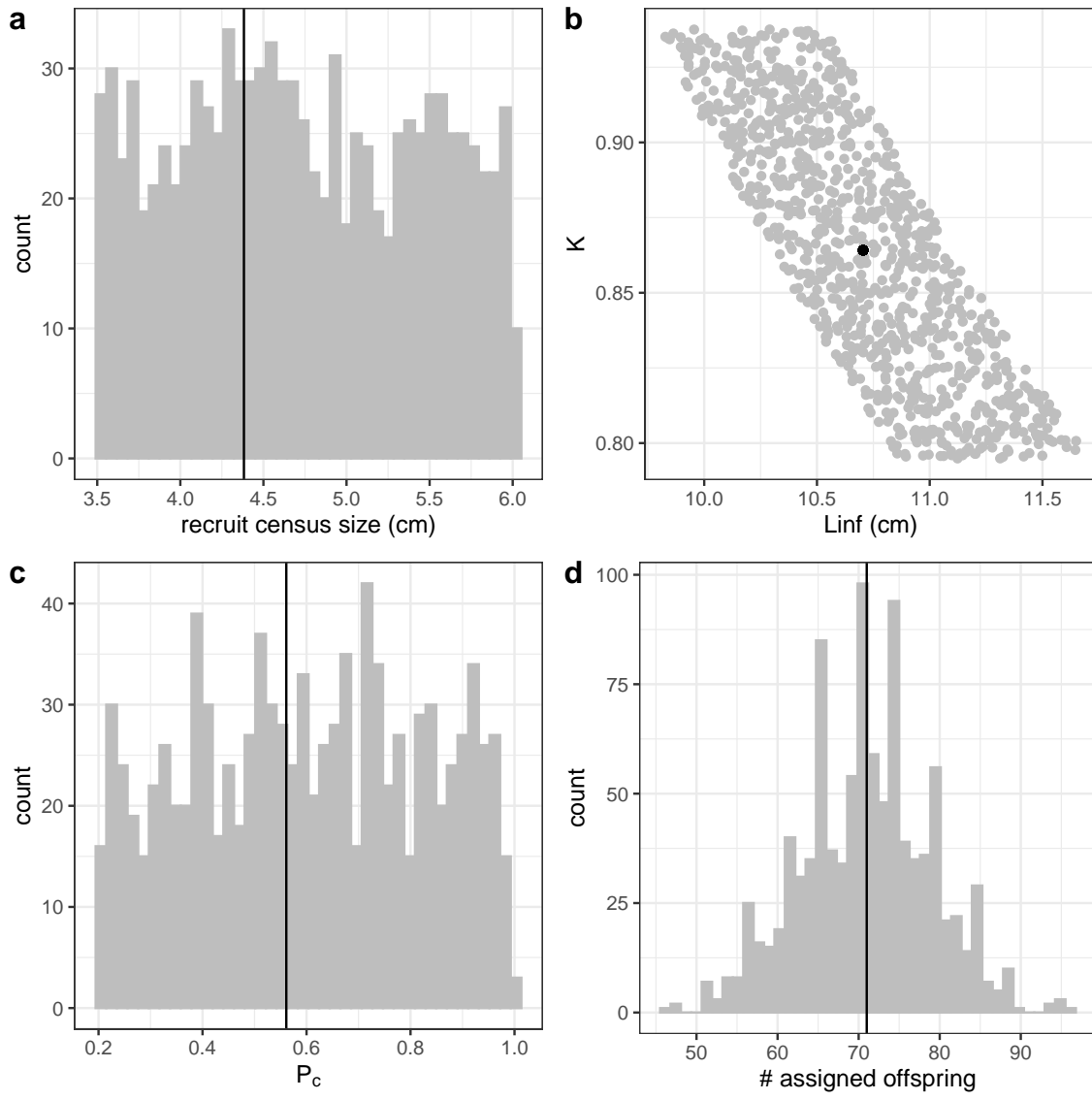


Figure D.3: Range of parameter inputs for uncertainty runs with all uncertainty included, where the black line or point is the value used for the best estimate: a)  $\text{size}_{\text{recruit}}$ , the census size for recruits after egg-recruit survival; b) the parameters  $L_{\infty}$  and  $k$  of the von Bertalanffy growth model; c)  $P_c$ , the probability of capturing a fish; d) number of offspring assigned back to parents in the parentage analysis.

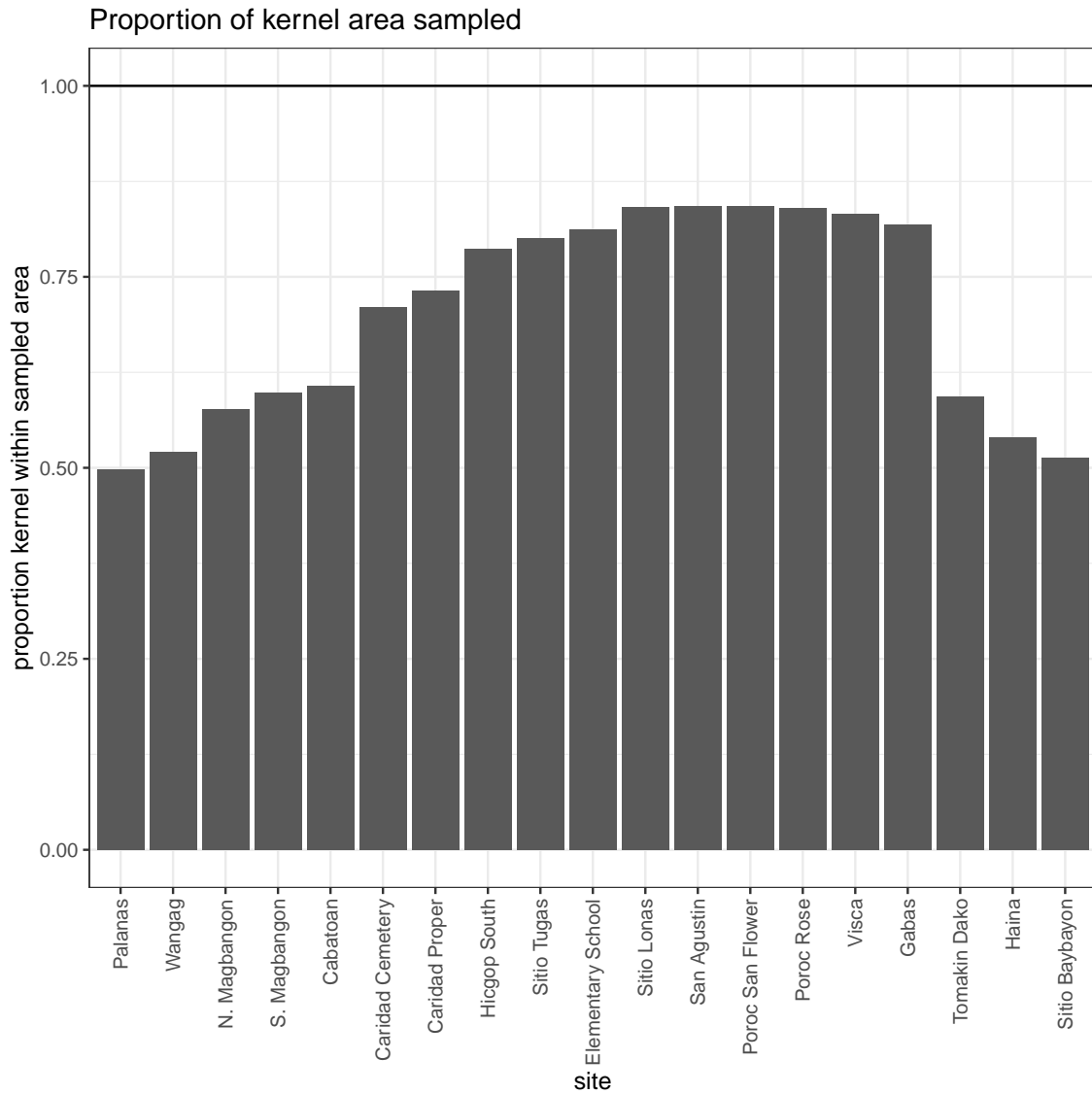


Figure D.4: Proportion of the dispersal kernel area from the center of each patch covered by our sampling region ( $\frac{A_i}{N_{g,i}}$  from eqn. A.3). The overall proportion ( $P_d$ ) is weighted by the number of parents at each patch.

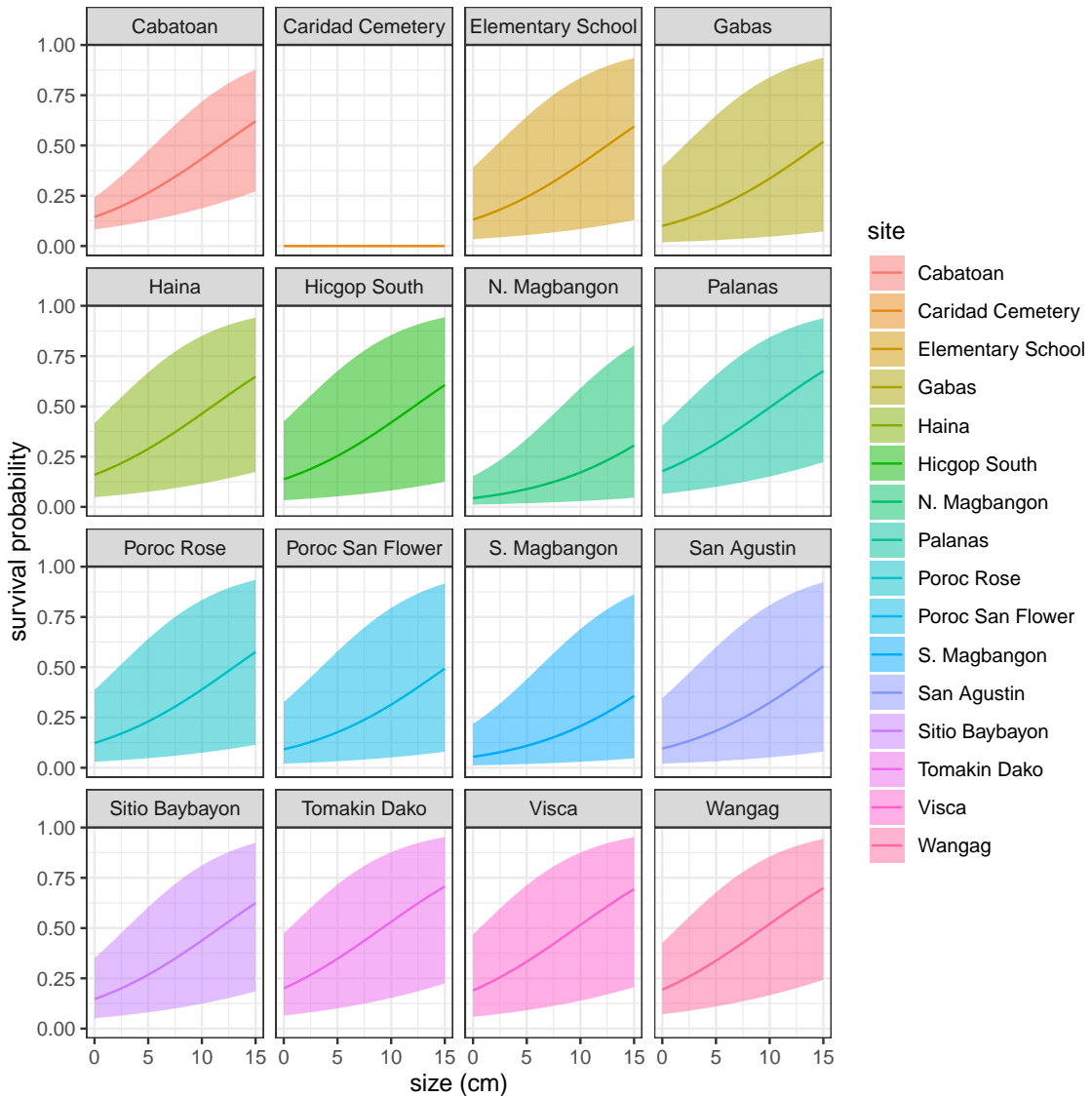


Figure D.5: Annual survival ( $\phi$ ) by fish size at each patch, detailed in SI A.3, A.9, and B.4.

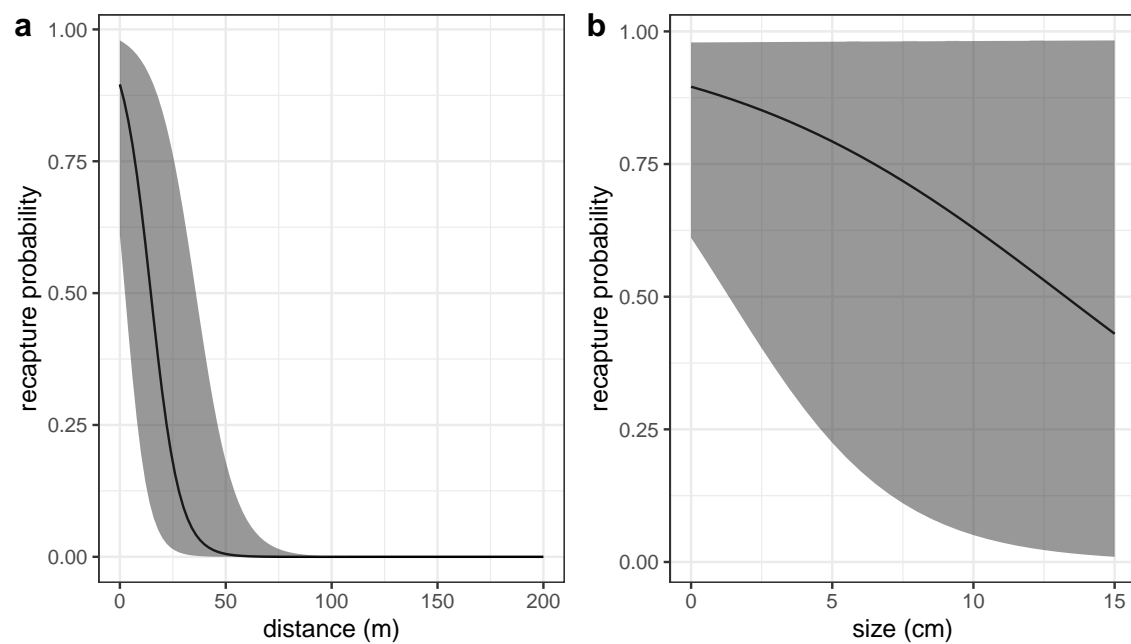


Figure D.6: Effects of a) minimum distance between divers and the anemone where the fish was first caught and b) fish size on recapture probability, estimated along with survival in a mark-recapture analysis (SI A.3, B.4).

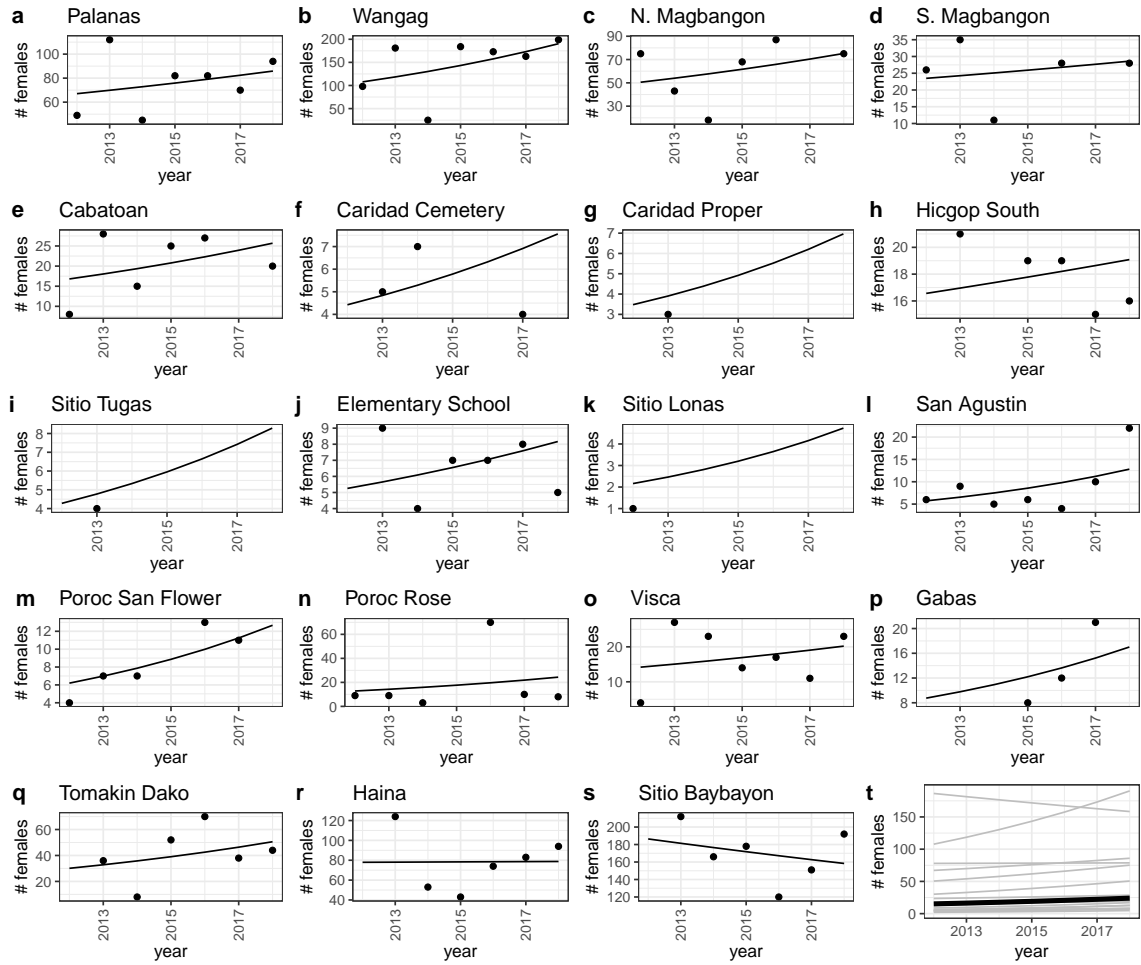


Figure D.7: Scaled number of females captured (black dots) and abundance trends (black lines) by patch from a mixed effects model with patch as a random effect.

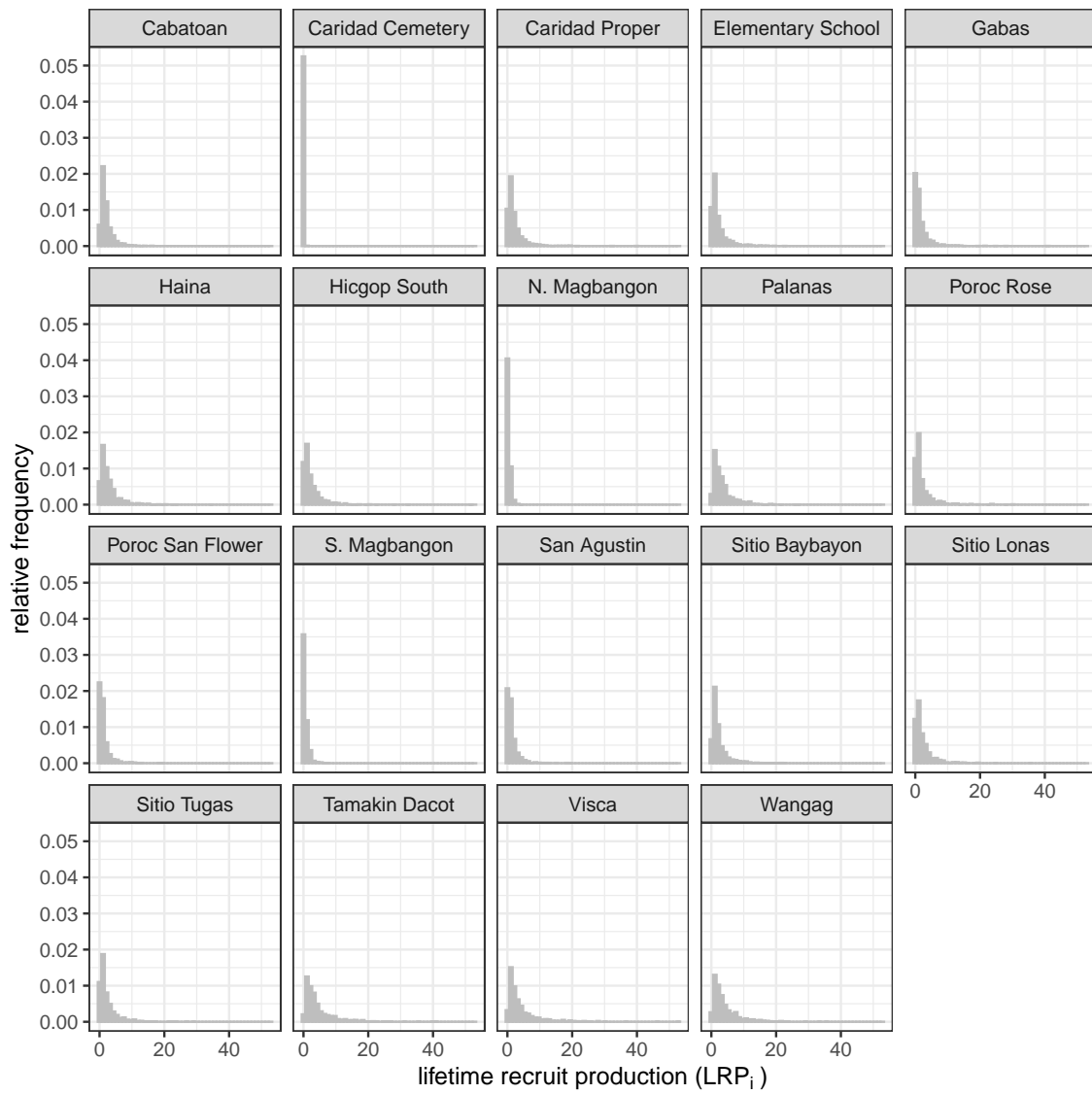


Figure D.8: Patch-specific lifetime recruit production ( $LRP_i$ ) estimates.

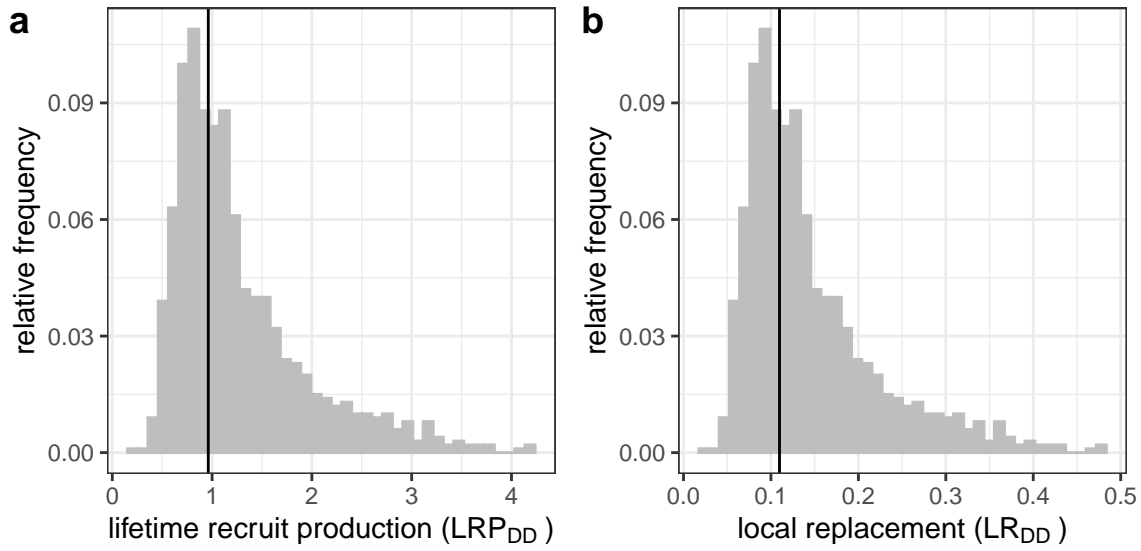


Figure D.9: Estimates of a) LRP averaged across patches, and b) local replacement without compensating for density dependence in early life stages in our data, showing the best estimate (black solid line) and range of estimates considering uncertainty (grey). These estimates compare to those in Fig. 4b and c, where we corrected for additional mortality in early life due to density dependence.

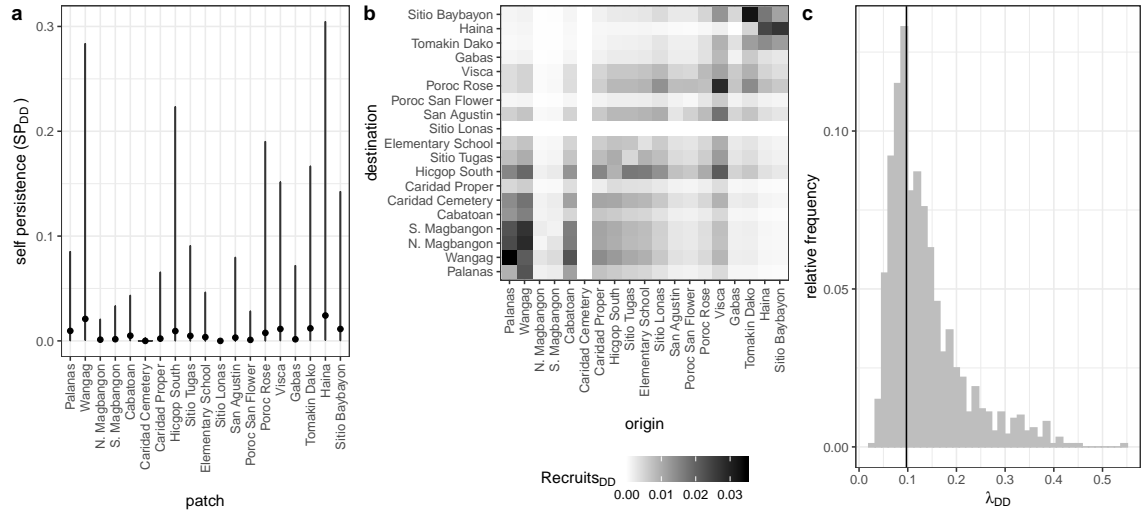


Figure D.10: Values of a) self-persistence ( $SP_{DD}$ ), b) realized connectivity among patches ( $C_{i,j,DD}$ ), and c) network persistence ( $\lambda_{c,DD}$ ) without compensation for density-dependence in early life stages in our data. For self-persistence (a) and network persistence (c), the best estimate is shown with in black (point for (a), line for (c)) and the range of estimates considering uncertainty is shown in grey. These estimates compare to those in Fig. 5 where we compensated for density dependence in early life stages.

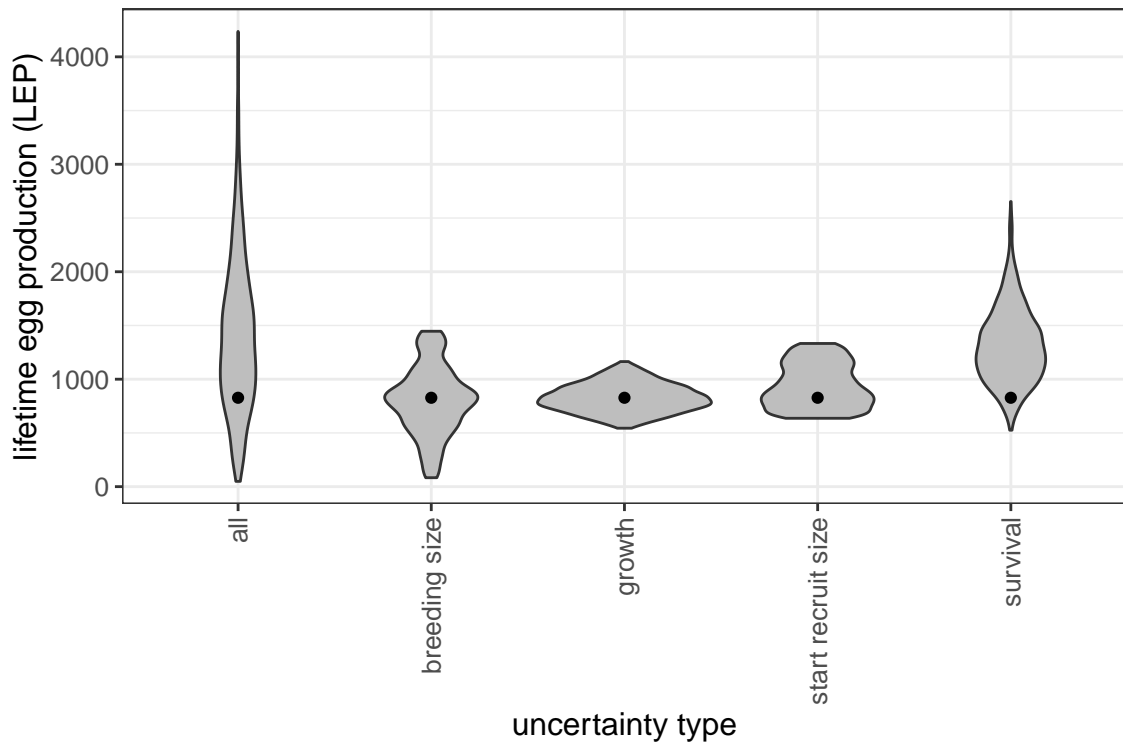


Figure D.11: The contribution of different sources of uncertainty in LEP averaged across patches ( $LEP_*$ ). We calculated the metrics using best estimates for all inputs except the one shown and show the results as violin plots, which show vertical probability densities of the metrics across a range of values.

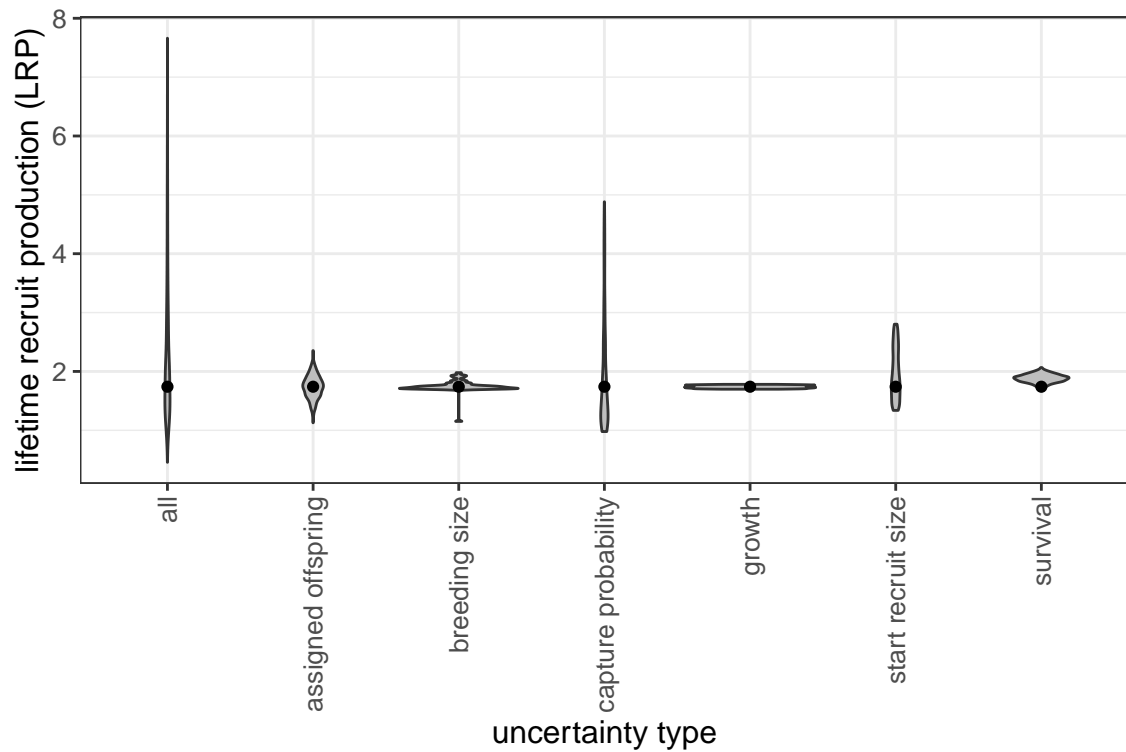


Figure D.12: The contribution of different sources of uncertainty in LRP. We calculated the metrics using best estimates for all inputs except the one shown and show the results as violin plots, which show vertical probability densities of the metrics across a range of values.

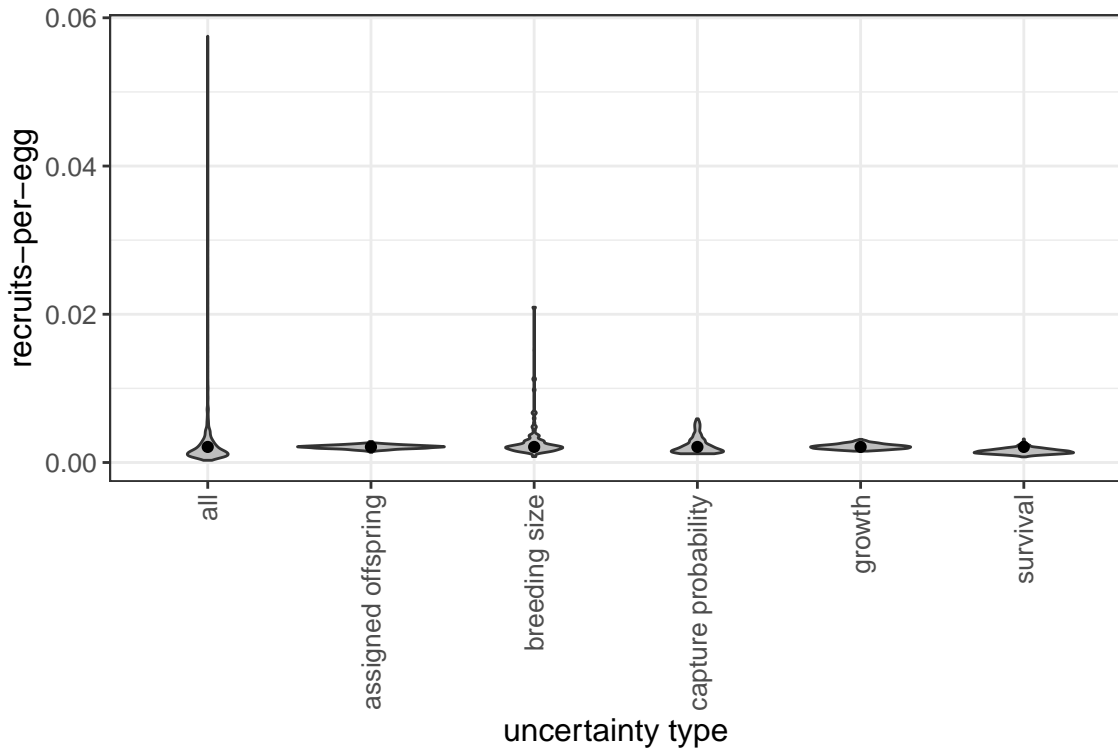


Figure D.13: The contribution of different sources of uncertainty in egg-recruit survival ( $S_e$ ). We calculated the metrics using best estimates for all inputs except the one shown and show the results as violin plots, which show vertical probability densities of the metrics across a range of values.

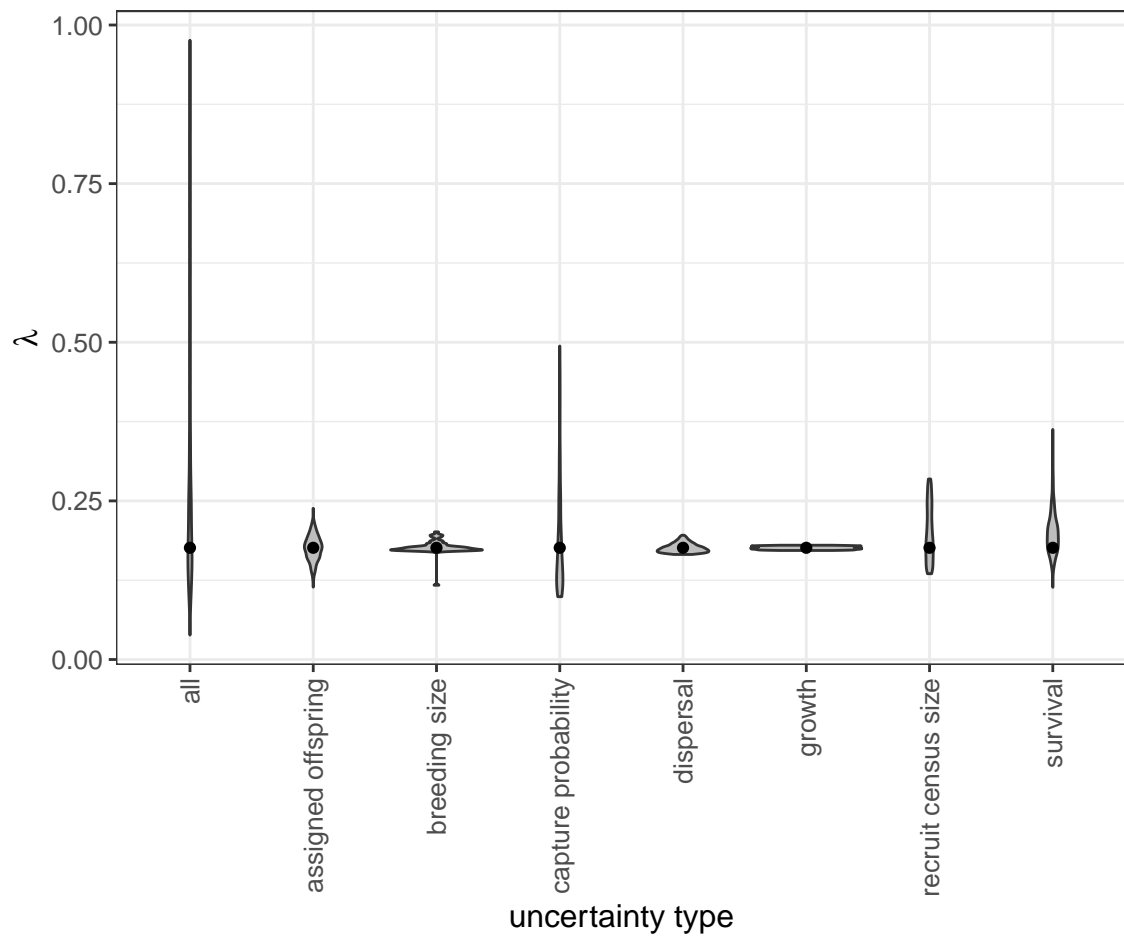


Figure D.14: The contribution of different sources of uncertainty in network persistence ( $\lambda_c$ ). We calculated the metrics using best estimates for all inputs except the one shown and show the results as violin plots, which show vertical probability densities of the metrics across a range of values.

## References

- 753 Almany, G. R., S. Planes, S. R. Thorrold, M. L. Berumen, M. Bode, P. Saenz-Agudelo, et al. (2017). Larval fish dispersal in a coral-reef seascape. *Nature Ecology & Evolution*, 1:0148.
- 756 Arvedlund, M., M. I. McCormick, D. G. Fautin, and M. Bildsøe. (1999). Host recognition and possible imprinting in the anemonefish *Amphiprion melanopus* (Pisces: Pomacentridae). *Marine Ecology Progress Series*, 188:207–218.
- 759 Baetscher, D. S., E. C. Anderson, E. A. Gilbert-Horvath, D. P. Malone, E. T. Saarman, M. H. Carr, et al. (2019). Dispersal of a nearshore marine fish connects marine reserves and adjacent fished areas along an open coast. *Molecular Ecology*, 28(7):1611–1623.
- 762 Bates, D., M. Mächler, B. Bolker, and S. Walker. (2015). Fitting linear mixed-effects models using lme4. *Journal of Statistical Software*, 67(1):1–48.
- 765 Bellwood, D. R. and R. Fisher. (2001). Relative swimming speeds in reef fish larvae. *Marine Ecology Progress Series*, 211:299–303.
- Bode, M., D. H. Williamson, H. B. Harrison, N. Outram, and G. P. Jones. (2018).  
768 Estimating dispersal kernels using genetic parentage data. *Methods in Ecology and Evolution*, 9(3):490–501.
- Bode, M., J. M. Leis, L. B. Mason, D. H. Williamson, H. B. Harrison, S. Choukroun,

771 and et al. (2019). Successful validation of a larval dispersal model using genetic  
parentage data. *PLOS Biology*, 17(7):1–13.

Botsford, L. W., A. Hastings, and S. D. Gaines. (2001). Dependence of sustainability  
774 on the configuration of marine reserves and larval dispersal distance. *Ecology  
Letters*, 4:144–150.

Botsford, L. W., J. W. White, and A. Hastings. (2019). *Population Dynamics for  
777 Conservation*. Oxford University Press.

Burgess, S. C., K. J. Nickols, C. D. Griesemer, L. A. K. Barnett, A. G. Dedrick,  
E. V. Satterthwaite, et al. (2014). Beyond connectivity: how empirical meth-  
780 ods can quantify population persistence to improve marine protected-area design.  
*Ecological Applications*, 24(2):257–270.

Buston, P. (2003a). Forcible eviction and prevention of recruitment in the clown  
783 anemonefish. *Behavioral Ecology*, 14(4):576–582.

Buston, P. (2003b). Social hierarchies: size and growth modification in clownfish.  
*Nature*, 424(6945):145–146.

786 Buston, P. M. and C. C. D'Aloia. (2013). Marine ecology: reaping the benefits of  
local dispersal. *Current Biology*, 23(9):R351–R353.

Buston, P. M. and J. Elith. (2011). Determinants of reproductive success in dominant  
789 pairs of clownfish: a boosted regression tree analysis. *Journal of Animal Ecology*,  
80(3):528–538.

- Buston, P. M., G. P. Jones, S. Planes, and S. R. Thorrold. (2011). Probability of  
792 successful larval dispersal declines fivefold over 1 km in a coral reef fish. *Proceedings  
of the Royal Society of London B: Biological Sciences*, p. rspb20112041.
- Carson, H. S., G. S. Cook, P. C. López-Duarte, and L. A. Levin. (2011). Evaluating  
795 the importance of demographic connectivity in a marine metapopulation. *Ecology*,  
92(10):1972–1984.
- Catalano, K. A., A. G. Dedrick, M. R. Stuart, J. Purtiz, H. R. Montes, Jr., and  
798 M. L. Pinsky. (in review). Quantifying dispersal variability among nearshore marine  
populations.
- Cinner, J. E., C. Huchery, M. A. MacNeil, N. A. J. Graham, T. R. McClanahan,  
801 J. Maina, et al. (2016). Bright spots among the world's coral reefs. *Nature*, 535  
(7612):416–419.
- Coleman, M. A., P. Cetina-Heredia, M. Roughan, M. Feng, E. Sebille, and B. P.  
804 Kelaher. (2017). Anticipating changes to future connectivity within a network of  
marine protected areas. *Global Change Biology*.
- D'Aloia, C. C., S. M. Bogdanowicz, J. E. Majoris, R. G. Harrison, and P. M. Buston.  
807 (2013). Self-recruitment in a Caribbean reef fish: a method for approximating  
dispersal kernels accounting for seascape. *Molecular Ecology*, 22(9):2563–2572.
- Elliott, J. K., J.M. Elliott, and R.N. Mariscal. (1995). Host selection, location, and  
810 association behaviors of anemonefishes in field settlement experiments. *Marine  
Biology*, 122(3):377–389.

- Ellner, S. P., D. Z. Childs, and M. Rees. (2016). Data-driven modelling of structured  
813 populations. *A practical guide to the Integral Projection Model*. Springer.
- Fahrig, L. (2001). How much habitat is enough? *Biological Conservation*, 100(1):  
65–74.
- 816 Fautin, D. G. and G. R. Allen. (1992). Field guide to anemonefishes and their host  
sea anemones. Western Australian Museum.
- Figueira, W. F. (2009). Connectivity or demography: defining sources and sinks in  
819 coral reef fish metapopulations. *Ecological Modelling*, 220(8):1126–1137.
- Figueira, W. F. and L. B. Crowder. (2006). Defining patch contribution in source-  
sink metapopulations: the importance of including dispersal and its relevance to  
822 marine systems. *Population Ecology*, 48(3):215–224.
- Figueira, W. F., S. J. Lyman, L. B. Crowder, and G. Rilov. (2008). Small-scale  
demographic variability of the bicolor damselfish, *Stegastes partitus*, in the Florida  
825 Keys, USA. *Environmental Biology of Fishes*, 81(3):297–311.
- Fisher, R. (2005). Swimming speeds of larval coral reef fishes: impacts on self-  
recruitment and dispersal. *Marine Ecology Progress Series*, 285:223–232.
- 828 Fuller, E., E. Brush, and M. L. Pinsky. (2015). The persistence of populations facing  
climate shifts and harvest. *Ecosphere*, 6(9):1–16.
- Garavelli, L., J. W. White, I. Chollett, and L. Marcel. (2018). Chérubin. Population

831 models reveal unexpected patterns of local persistence despite widespread larval  
dispersal in a highly exploited species. *Conservation Letters*, 11(5):e12567.

Hameed, S. O., J. W. White, S. H. Miller, K. J. Nickols, and S. G. Morgan. (2016).  
834 Inverse approach to estimating larval dispersal reveals limited population connec-  
tivity along 700 km of wave-swept open coast. *Proceedings of the Royal Society B:  
Biological Sciences*, 283(1833):20160370.

837 Hanski, I. (1998). Metapopulation dynamics. *Nature*, 396(6706):41–49.

Harms, K. E., S. J. Wright, O. Calderón, A. Hernandez, and E. A. Herre. (2000).  
Pervasive density-dependent recruitment enhances seedling diversity in a tropical  
840 forest. *Nature*, 404(6777):493–495.

Hart, D. R. and A. S. Chute. (2009). Estimating von Bertalanffy growth parameters  
from growth increment data using a linear mixed-effects model, with an application  
843 to the sea scallop *Placopecten magellanicus*. *ICES Journal of Marine Science*, 66  
(10):2165–2175.

Hastings, A. and L. W. Botsford. (2006). Persistence of spatial populations depends  
846 on returning home. *Proceedings of the National Academy of Sciences*, 103:6067–  
6072.

Hattori, A. and Y. Yanagisawa. (1991). Life-history pathways in relation to gonadal  
849 sex differentiation in the anemonefish, *Amphiprion clarkii*, in temperate waters of  
Japan. *Environmental Biology of Fishes*, 31(2):139–155.

- Hayashi, K., K. Tachihara, and J. D. Reimer. (2019). Low density populations  
852 of anemonefish with low replenishment rates on a reef edge with anthropogenic  
impacts. *Environmental Biology of Fishes*, 102(1):41–54.
- Hijmans, R. J. (2017). *geosphere: Spherical Trigonometry*. R package version 1.5-7.  
855 Holtswarth, J. N. S. B. San Jose, H. R. Montes Jr., J. W. Morley, and M. L Pin-  
sky. (2017). The reproductive seasonality and fecundity of yellowtail clownfish  
(*Amphiprion clarkii*) in the Philippines. *Bulletin of Marine Science*, 93.
- Johnson, D. W., M. R. Christie, T. J. Pusack, C. D. Stallings, and M. A. Hixon.  
858 (2018). Integrating larval connectivity with local demography reveals regional  
dynamics of a marine metapopulation. *Ecology*, 99(6):1419–1429.
- Kaplan, D. M., L. W. Botsford, M. R. O’Farrell, S. D. Gaines, and S. Jorgensen.  
861 (2009). Model-based assessment of persistence in proposed marine protected area  
designs. *Ecological Applications*, 19(2):433–448.
- Kritzer, J. P. and P. F. Sale. (2006). *Marine Metapopulations*. Elsevier Academic  
Press.  
864
- Laake, J. L. (2013). RMark: An R interface for analysis of capture-recapture data  
with MARK. R package version 2.2.6.  
867
- Lecchini, D., S. Planes, and R. Galzin. (2005). Experimental assessment of sensory  
modalities of coral-reef fish larvae in the recognition of their settlement habitat.  
870 *Behavioral Ecology and Sociobiology*, 58(1):18–26.

- Moilanen, A., A. T. Smith, and I. Hanski. (1998), Long-term dynamics in a metapopulation of the American pika. *The American Naturalist*, 152(4):530–542.
- 873 Moyer, J. T. (1976). Geographical variation and social dominance in Japanese populations of the anemonefish *Amphiprion clarkii*. *Japanese Journal of Ichthyology*, 23(1):12–22.
- 876 Nowicki, P. and V. Vrabec. (2011). Evidence for positive density-dependent emigration in butterfly metapopulations. *Oecologia*, 167(3):657.
- 879 Nowicki, P., S. Bonelli, F. Barbero, and E. Balletto. (2009). Relative importance of density-dependent regulation and environmental stochasticity for butterfly population dynamics. *Oecologia*, 161(2):227–239.
- 882 Ochi, H. (1989). Mating behavior and sex change of the anemonefish, *Amphiprion clarkii*, in the temperate waters of southern Japan. *Environmental Biology of Fishes*, 26(4):257–275.
- Pinsky, M. L., H. R. Montes Jr, and S. R. Palumbi. (2010). Using isolation by distance and effective density to estimate dispersal scales in anemonefish. *Evolution*, 64(9):2688–2700.
- 888 Puckett, B. J. and D. B. Eggleston. (2016). Metapopulation dynamics guide marine reserve design: importance of connectivity, demographics, and stock enhancement. *Ecosphere*, 7(6).

- Pulliam, H. R. (1988). Sources, sinks, and population regulation. *The American Naturalist*, 132(5):652–661.
- Rodenhouse, N. L., T. S. Sillett, P. J. Doran, and R. T. Holmes. (2003), Multiple density-dependence mechanisms regulate a migratory bird population during the breeding season. *Proceedings of the Royal Society of London. Series B: Biological Sciences*, 270(1529):2105–2110.
- Sale, P. F., I. Hanski, and J. P. Kritzer. (2006). The merging of metapopulation theory and marine ecology: establishing the historical context. In *Marine Metapopulations*, pp. 3–28. Elsevier.
- Salles, O. C., G. R. Almany, M. L. Berumen, G. P. Jones, P. Saenz-Agudelo, M. Srinivasan, et al. (2020). Strong habitat and weak genetic effects shape the lifetime reproductive success in a wild clownfish population. *Ecology Letters*, 23(2):265–273.
- Salles, O. C., J. A. Maynard, M. Joannides, C. M. Barbu, P. Saenz-Agudelo, G. R. Almany, et al. (2015). Coral reef fish populations can persist without immigration. *Proceedings of the Royal Society B: Biological Sciences*, 282(1819):20151311.
- Smedbol, R. K., A. McPherson, M. M. Hansen, and E. Kenchington. (2002). Myths and moderation in marine metapopulations? *Fish and Fisheries*, 3(1):20–35.
- Smith, J. N. M. and J. J. Hellmann. (2002). Population persistence in fragmented landscapes. *Trends in Ecology & Evolution*, 17(9):397–399.

- Thompson, D. M., J. Kleypas, F. Castruccio, E. N. Curchitser, M. L. Pinsky,  
B. Jönsson, et al. (2018). Variability in oceanographic barriers to coral larval  
912 dispersal: Do currents shape biodiversity? *Progress in Oceanography*, 165:110–  
122.
- Tolimieri, N. and P. S. Levin. (2005). The roles of fishing and climate in the popu-  
915 lation dynamics of bocaccio rockfish. *Ecological Applications*, 15(2):458–468.
- Vermeij, M. J. A. and S. A. Sandin. (2008). Density-dependent settlement and  
mortality structure the earliest life phases of a coral population. *Ecology*, 89(7):  
918 1994–2004.
- Warner, R. R. and P. L. Chesson. (1985). Coexistence mediated by recruitment  
fluctuations: a field guide to the storage effect. *The American Naturalist*, 125(6):  
921 769–787.
- Warner, R. R. and T. P. Hughes. (1988). The population dynamics of reef fishes.  
6th International Coral Reef Symposium Executive Committee.
- 924 White, J. W. and J. F. Samhouri. (2011). Oceanographic coupling across three  
trophic levels shapes source–sink dynamics in marine metacommunities. *Oikos*,  
120(8):1151–1164.
- 927 White, J. W., M. H. Carr, J. E. Caselle, L. Washburn, C. B. Woodson, S. R. Palumbi,  
et al. (2019). Connectivity, dispersal, and recruitment: Connecting benthic com-  
munities and the coastal ocean. *Oceanography*, 32(3):50–59.

- 930 White, J. W., L. W. Botsford, A. Hastings, and J. L. Largier. (2010). Population persistence in marine reserve networks: incorporating spatial heterogeneities in larval dispersal. *Marine Ecology Progress Series*, 398:49–67.